

TU Delft Thesis

Seismic Resilience Assessment of Water
Distribution Networks
Optimization of the Recovery Process and
Characteristic Curves

MSc Construction Management Engineering
Vasiliki Tsioni

Seismic Resilience Assessment of Water Distribution Networks Optimization of the Recovery Process and Characteristic Curves

A thesis submitted to the Delft University of Technology in partial fulfillment
of the requirements for the degree of

Master of Science in Construction Management and Engineering
Faculty of Engineering & Geosciences

by

Vasiliki Tsioni

Student Number: 5160944

Thesis Committee:

Dr.ir. M. (Maria) Nogal Macho
Dr Omar Kammouh

Graduation Chair, TU Delft
Main Supervisor, TU Delft

Preface

This thesis concludes my studies in the master's program of Construction Management and Engineering of TU Delft. The research presented here is inspired by my interest in the field of resilience within the civil infrastructure domain. Water distribution networks (WDNs) represent a critical infrastructure, essential for sustaining urban life. However, they are highly susceptible to damage during earthquakes, underscoring the need for a deeper understanding of their resilience.

To address this challenge, an optimization model was developed to simulate and optimize the pipeline recovery sequence of WDNs. The results of this optimization were used to derive characteristic curves of the network, providing an innovative tool for evaluating WDN resilience. These characteristic curves allow for a detailed assessment of a network's ability to recover from disruptions while maintaining its functionality. This work offers decision-makers a practical and scalable tool that can be applied to networks of various sizes and implemented in real-life scenarios. By utilizing this tool, decision-makers are better equipped to respond to disasters, enhancing the resilience of WDNs.

I would like to express my gratitude to my supervisors, Dr. Ir. Maria Nogal Macho and Dr. Omar Kammouh, for their invaluable guidance and support throughout this process. Their insights and advice were instrumental in shaping this thesis. I also extend my deepest appreciation to my friends and family for their understanding and encouragement during this time.

Vasiliki Tsioni
Delft, January 2025

Summary

The resilience of civil infrastructure has emerged as a prominent research field in recent years. Aging infrastructure, combined with unexpected hazards, presents challenges to the civil domain that were often not anticipated during their design phase. Water distribution networks (WDNs), as a core component of civil infrastructure, are integral to sustaining urban life. Spanning large areas and comprising multiple interdependent components, WDNs are particularly susceptible to natural hazards. While considerable research has been conducted on the resilience of WDN design, studies focusing on their resilience under seismic conditions remain scarce.

This thesis delves into the area of seismic resilience in WDNs, with an emphasis on the post-earthquake recovery phase. It proposes an easy-to-implement optimization model aimed at enhancing the resilience of WDNs following seismic disruptions. By incorporating hydraulic simulations, this model aims to strike a balance between practicality and computational efficiency. The goal is to provide asset managers with a tool that does not require high computational resources, yet avoids oversimplification, ensuring real-world applicability.

Building on the optimization model, the research introduces the concept of characteristic curves for WDNs. These performance curves are generated by analyzing the network under various earthquake magnitudes and resource availability scenarios. These curves offer a scenario-independent evaluation of network resilience, providing a visual and intuitive representation of its performance. This innovative tool enables decision-makers to make swift and informed choices during disaster response, while also supporting proactive preparedness efforts.

The final chapter of the thesis reflects on the limitations of the research and its practical implications for construction management. It also provides recommendations for future research. Key limitations include the use of a static resource allocation and the application to real-life urban WDNs where the assumptions of the model will reflect reality. Future research can significantly advance resilience planning by incorporating dynamic resource strategies. The introduction of appropriate thresholds for different damage levels could also be incorporated in the expansion of the characteristic curves, allowing for effective resilience planning.

Contents

Preface	i
Summary	ii
1 Introduction	1
1.1 Problem Statement	1
1.2 Research Gap	1
1.3 Objectives	1
1.4 Research Question	2
1.5 Research Relevance	2
1.6 Practical Relevance	2
1.7 Thesis Outline	3
2 Seismic Resilience Assessment of Water Distribution Networks; Optimization of the Recovery Process and Characteristic Curves	4
3 Conclusions	5
3.1 Response to Research Questions	5
3.2 Research Limitations	7
3.3 Reflection & Connection to the CME program	7
References	9

1

Introduction

1.1. Problem Statement

Water distribution networks (WDNs) are critical infrastructure systems that are responsible for securing adequate quantities of safe, high-quality water to the public [2]. Their resilience is defined as the ability to withstand, adapt to, and rapidly recover from the effects of a disruptive event [4]. In the event of a catastrophic earthquake, WDNs need to recover quickly and provide water as well as assist in firefighting and other rescue operations. Given the unpredictability in the occurrence and magnitude of earthquakes, along with the complex interdependence of the sub-components of the networks, the recovery process of WDNs proves to be challenging. This work aims to provide an assessment on the resilience of WDNs by optimizing the recovery process under different seismic scenarios.

1.2. Research Gap

The majority of research on WDNs focuses on achieving optimality during the design phase of the infrastructure. However, aging and deterioration of WDNs increase their vulnerability and the likelihood of function interruption during and after disruptive events such as natural hazards [2]. Earthquakes, floods and extreme weather events due to climate change are examples of natural hazards that can threaten the infrastructure system. Scientific research on the recovery - based seismic resilience of WDNs is scant. Instead, the focus the last two decades has been on the assessment of the resilience of WDNs by defining metrics that will be able to encapsulate the meaning of resilience and provide generalized assessments of the state of WDNs under normal operations. However, a unified definition of WDN resilience appears to be lacking in the literature [9]. That results in several different metrics being developed and tested in scientific research [2, 4, 15, 12, 3, 5, 7, 10, 8]. In terms of recovery based resilience, the research has been focused on simulating the recovery activities and comparing different recovery strategies [13]. Discrete event simulation model (DESM) has been used to study the recovery process under different stress scenarios [14]. The components of the WDNs such as tanks and pumps, were also examined in assessing their role in different recovery strategies [4]. Optimization of the recovery sequence of pipes as a means of assessing the seismic resilience of the WDNs has only been introduced recently by [13]. The metric that is used to assess the performance of the system is a satisfaction degree index (SDI) and different recovery strategies were examined which lead to different values of the metric.

1.3. Objectives

The research field of recovery based seismic resilience of WDNs is still largely unexplored. As a key aspect of their resilience, the recovery process after a seismic event needs to be optimized in order to avoid large direct and indirect losses. Furthermore, since no seismic event is ever the same, the system needs to be resilient in a non-case dependent way. That leads us to attempt at creating an assessment tool for the resilience of WDNs, based on the recovery process under several seismic

events.

1.4. Research Question

Based on the research gaps and the objectives of this work, as they were presented in the previous section the main research question is formulated as follows:

Main Research Question

Can we provide a scenario - free assessment of the recovery based seismic resilience of WDNs, by the identification of characteristic curves for system recovery?

The 3 sub-questions that are going to guide us in the effort to answer the main question are:

1. What is the appropriate metric for the assessment of the recovery-based seismic resilience of WDNs?
2. How can we optimize the recovery process of the examined WDN under the different stress scenarios and resource constraints?
3. How can we extend the results of the optimization process by identifying the characteristic curves of the system?

1.5. Research Relevance

This work focuses on the research field of post-earthquake recovery of water distribution networks (WDNs). The resilience of WDNs is evaluated through a simulation-based optimization model of the pipeline infrastructure, given its critical role in the recovery process, as highlighted in relevant literature [13, 9, 6]. Building on this foundation, the research aims to extend the applicability of the optimization model by examining its performance under varying earthquake magnitudes and resource availability scenarios. The outcomes are presented as characteristic curves, which provide a novel, scenario-independent method for assessing the resilience of WDNs.

The introduction of characteristic curves for resilience assessment seeks to advance research on the post-recovery resilience of WDNs. By offering a performance evaluation framework that is not tied to specific scenarios, this approach provides a more comprehensive understanding of WDN recovery capabilities, contributing valuable insights for both academic research and practical decision-making.

1.6. Practical Relevance

In aligning this research with current practices within the WDNs community, the proposed model aspires to be practical and accessible for practitioners. The aim is the optimization model developed to be easily applicable and achieve accurate results in the recovery process of the pipeline infrastructure, while maintaining a strong scientific foundation that reflects the hydraulic complexities of WDNs. The introduction of characteristic curves as a second phase of the optimization model is designed to appeal to asset managers, engineers, and decision-makers. These curves provide an intuitive and visual representation of the overall resilience behavior of WDNs following an earthquake event. By offering a clear depiction of network performance, the characteristic curves serve as an easy-to-understand tool for decision-makers, facilitating enhanced preparedness efforts. Moreover, they promote a deeper understanding of the relationship between resilience targets and the resources required to achieve them.

Policymakers may also benefit from the insights and conclusions of this work in their efforts to prepare for or mitigate the impacts of earthquakes. By offering practical tools and actionable findings, this research bridges the gap between scientific advancements and real-world applications, contributing to the resilience and recovery of WDNs. However, this thesis also acknowledges several limitations. The proposed optimization model is computationally intensive, especially when applied to large-scale networks. Additionally, the study is based on predefined resource availability and earthquake scenarios, which can differ in real life cases scenarios. Lastly, while the research is tailored for seismic recovery, its applicability to other types of hazards or multi-hazard scenarios remains unexplored. Extending the work to accommodate different hazard profiles would enhance its versatility and practical relevance.

1.7. Thesis Outline

This paper-based thesis is structured into three main chapters. Chapter 1 introduces the problem statement, the research gap, the objectives, the research questions and the practical and research relevance of the study. The research paper is presented in the second chapter and includes the optimization model and the characteristic curves for different scales of networks as well as their characterization and conclusions on overall resilience performance. Finally, Chapter 3 concludes the research findings, acknowledges its limitations, and discusses how this study fits into the larger framework of the field of construction management.

2

Seismic Resilience Assessment of Water Distribution Networks; Optimization of the Recovery Process and Characteristic Curves

This chapter presents the main research paper of the thesis. It begins by introducing the resilience metric selected based on a review of the existing literature. Subsequently, it delves into the mathematical formulation of the optimization model. Following the implementation of the optimization model, the production of characteristic curves is presented. These curves are derived from the results of the optimization and serve as an evaluating tool for resilience. To assess the applicability of the model, networks of different scales are analyzed, and their respective results are discussed. The conclusions drawn from the research paper provide valuable insights into the resilience of WDNs during the post-seismic recovery phase. By aligning closely with the objectives and research questions outlined in the introduction, this paper serves as the foundation of the thesis and underscores its contribution to the field.

Seismic Resilience Assessment of Water Distribution Networks; Optimization of the Recovery Process and Characteristic Curves

V. Tsioni^{a,*}, O. Kammouh^a, M. Nogal^a

^a*Faculty of Civil Engineering & Geosciences, Delft University of Technology, Netherlands*

Abstract

Water Distribution Networks (WDNs) play a pivotal role in maintaining urban resilience, especially in the aftermath of seismic disruptions. Despite their importance, existing resilience assessments for these systems face limitations, including the lack of a consensus on the definition of resilience and insufficient emphasis on the recovery process. This study evaluates the seismic resilience of WDNs by developing an optimization model to prioritize pipeline repair sequences. The optimized sequence is then used to generate the characteristic curves of the network, offering an assessment on its overall performance. The optimization is carried out using a Genetic Algorithm, while various scenarios of seismic intensities and available resources are considered to generate the characteristic curves. To assess scalability and broad applicability, the model is tested on WDNs of varying sizes. The results offer key insights into the resilience of WDNs, reflecting their intrinsic behavior under seismic stress. This integrated approach—linking resource distribution, repair scheduling, and resilience metrics—can guide asset managers, engineers, and policymakers in both risk management and recovery planning for WDNs in seismic-prone regions.

Keywords: Water Distribution Networks, resilience, optimization, recovery sequence, characteristic curves

1. Introduction

Water Distribution Networks (WDNs) form a core component of critical infrastructure. According to the National Protection Plan, critical infrastructures are the backbone of resilient cities; their incapacitation or destruction could severely impact security, the economy, public health, safety, and the environment [1]. WDNs, specifically, ensure the supply of safe, high-quality water to the public, playing an indispensable role in public health and safety [2].

*Corresponding author

They support industrial demands, facilitate economic growth, and are crucial for firefighting and rescue operations, contributing to urban and natural area preservation.

However, their complex and interconnected nature makes them vulnerable to both natural and human-made disasters. With components spanning large areas - often buried beneath urban infrastructure - these systems are particularly susceptible to natural hazards like earthquakes. Seismic waves can damage pipelines through soil - pipe interaction, potentially affecting large areas that are difficult to isolate and repair. Furthermore, WDNs rely heavily on other critical infrastructure systems, such as transportation networks and electrical grids [3]. Disruptions in these interdependent systems can cascade, further compromising WDNs' functionality.

The inherent uncertainty surrounding natural hazards, such as earthquakes, combined with the direct and indirect impacts on WDNs, presents significant challenges for asset owners tasked with ensuring functionality.

1.1. Literature Review

Traditional risk management approaches have primarily focused on physical asset protection to mitigate the impact of hazards, aiming to quantify risks and reduce consequences [4]. These methods, however, often assume predictable and measurable threats, an assumption that fails under the unpredictable nature of disasters like earthquakes. To address these limitations, the past two decades have witnessed a shift toward resilience-based approaches. Resilience, defined as a system's ability to prepare for, adapt to, and recover from disruptive events [1], emphasizes not just damage prevention but also the capacity to maintain functionality before, during and after a hazard. Nevertheless, resilience remains a somewhat ambiguous concept, with no universal scientific consensus on its definition [5]. Consequently, various methodologies have been developed to assess WDNs' resilience, which can be broadly categorized into two main approaches: the surrogate measure approach and the simulation of recovery strategies.

The surrogate measure approach employs metrics that indirectly quantify resilience by evaluating network properties such as hydraulic redundancy, structural robustness and topological attributes. One of the most widely recognized energy-based surrogate metrics is the Resilience Index, introduced by [6]. This metric quantifies the surplus hydraulic power available in a network relative to the minimum power required to deliver water at acceptable pressures, emphasizing hydraulic redundancy [6]. While particularly useful for looped networks, its applicability diminishes in non-looped or sparse networks with inherently low redundancy. Building on this concept, [7] incorporated measures of loop diameter uniformity, combining hydraulic performance and structural reliability to extend its utility. Similarly, [8] expanded surrogate metrics to account for pressure deficits and pipe redundancy, balancing cost efficiency with reliability. Despite these advancements, energy-based metrics often oversimplify the dynamic interactions between hydraulic, structural, and operational factors, which limits their effectiveness under extreme conditions.

Entropy-based methods offer an alternative by focusing on flow distribution and redundancy within the network. [9] employed Shannon Entropy to assess the randomness and uniformity of flow. Higher entropy values indicate greater adaptability and robustness, reflecting increased flow redundancy. [10] extended this concept with the Tsallis entropy, which captures non-linear relationships in flow variability and offers a more nuanced view of network performance. Although entropy-based metrics are intuitive and computationally straightforward, they often oversimplify hydraulic behavior and neglect structural and economic considerations.

Graph theory provides a structural perspective on resilience by modeling WDNs as mathematical graphs $G = (N, E)$, where N represents nodes (consumers and sources) and E represents edges (pipes). Metrics such as connectivity, clustering coefficients, and betweenness centrality are used to evaluate the robustness of the network. [11] emphasized the importance of topological redundancy and connectivity, demonstrating that networks with higher clustering coefficients are more resilient to localized failures. [12] highlighted critical nodes and edges by analyzing topological attributes like betweenness centrality, which identifies bottlenecks in flow. [13] proposed a framework for sectorized WDNs, emphasizing modularity and inter-sector connectivity to enhance resilience. Although graph theory metrics provide valuable insights into network structure, they often fail to integrate hydraulic and operational dynamics, critical for comprehensive resilience assessments.

Despite their widespread use, surrogate metrics face several significant limitations. Energy-based approaches, such as the Resilience Index, often overlook the interplay between hydraulic, structural, and operational factors under extreme conditions, leading to an incomplete representation of system’s resilience [6, 8]. Entropy-based methods provide valuable insights into flow distribution; however, they do not adequately incorporate structural and economic considerations, reducing their applicability to real-world scenarios [9, 10]. Similarly, graph theory metrics emphasize structural robustness but do not account for essential hydraulic properties, such as pressure and flow variability, which are crucial for evaluating operational performance [11, 12, 13]. In addition, most surrogate metrics are static and do not capture the temporal evolution of recovery processes. They often assume idealized conditions, ignoring real-world complexities such as repair prioritization, resource allocation, and inter-dependencies between infrastructure systems. For example, metrics like the Resilience Index or Shannon Entropy cannot adequately represent the cascading effects of disruptions across interdependent systems, a limitation noted by [14] and [15]. Moreover, the computational simplicity of these metrics often comes at the expense of accuracy and reliability under dynamic or extreme conditions, as highlighted by [5, 16].

The second approach that can be found in the field, focuses on the simulation of post-recovery processes as a means of assessing the resilience of WDNs. These simulation-based approaches emphasize the temporal evolution of recovery efforts following disruptive events, with particular attention to the relationship between repair strategies, resource allocation, and system performance. They

offer a dynamic perspective by modeling recovery in real-time and offer a resilience evaluation based on how effectively and quickly a network can restore its functionality.

[17] made use of Discrete Event Simulation Models (DESMs) for WDNs, simulating key recovery activities such as pipeline inspection, isolation, and repair scheduling. Their approach underscored the importance of repair sequencing to minimize service disruptions and recovery time. However, DESMs are often computationally intensive and depend on detailed data inputs, including pipeline damage states and repair resource capacities, which can restrict the model's scalability. Building on this framework, [15] incorporated resilience metrics into the DESM paradigm, explicitly linking recovery processes to system performance. Their model captured the complex inter-dependencies among infrastructure components, such as interactions between damaged pipelines and supporting systems like power and transportation networks. While this approach provided a more realistic depiction of recovery dynamics, it also increased computational complexity.

Other studies have taken a more targeted approach to resilience enhancement by investigating specific interventions. [18] examined strategies like ductile retrofitting and network meshing to mitigate damages during seismic events and accelerate subsequent recoveries, underscoring structural robustness as a vital component of overall resilience. Additionally, [19] evaluated seismic upgrades to pumps, considering both technical and organizational dimensions of resilience. Similarly, [20] introduced a resilience index that integrates factors such as user demand, system capacity (measured by tank height), and water quality, underscoring the importance of coordinated restoration efforts.

In addition to dynamic simulations of key restorative activities, optimization frameworks have been developed to identify effective recovery strategies. [21] introduces a resilience-based framework for decision-making that uses optimization, focusing on how to coordinate interventions under constrained budgets and uncertain seismic conditions. While the integrated approach promises more robust decisions compared to static strategies, it requires iterative interventions whenever new damage data become available. [14] integrated hydraulic simulations into recovery modeling to assess the impact of repair sequencing on flow distribution and pressure variability. Their study revealed critical bottlenecks that hinder recovery by combining hydraulic and structural analyses. Despite these insights, the dual-layer approach significantly increased computational demands, posing challenges for large-scale or real-time applications. [5], for instance, proposed a recovery-based optimization model that evaluates repair prioritization strategies, including those based on damage severity, proximity, or demand criticality. Their findings revealed that adaptive recovery strategies - where repair plans are dynamically adjusted based on evolving conditions - outperform static approaches. However, dynamic optimization often entails significant computational load, making it challenging to apply to large-scale networks.

Studies by [2, 5, 14, 16], emphasized damaged pipelines as the primary bottleneck to restoring water services after earthquakes. [16] introduced phased recov-

ery schedules, incorporating differentiated user priorities, progressive restoration of service levels, and variable demand patterns. Their framework explicitly modeled the gradual recovery of WDN functionality, closely aligning with real-world scenarios. This approach offered valuable insights into the dynamic interplay between user demands and repair processes. However, it relied on granular data, such as household-level consumption patterns and pipeline-specific damage assessments, which can limit its applicability in regions lacking detailed data infrastructure.

While simulation-based approaches represent significant advancements over static metrics in assessing the resilience of WDNs, there are still challenges to be addressed. One prominent challenge lies in the scalability of dynamic recovery models. These models often struggle to accommodate large, complex networks due to their computational intensity. For example, the frameworks developed by [5, 15] require substantial processing power to simulate recovery scenarios on a large scale, rendering them impractical for real-time decision-making in many cases. Another critical limitation is the dependence on high-resolution data. Recovery simulations typically require detailed inputs, such as fragility curves, repair crew schedules, and real-time demand patterns, to generate accurate results. However, such data is frequently unavailable or unreliable, especially in resource-constrained or disaster-affected regions, as highlighted by [14]. This data dependency restricts the applicability of simulation-based models in areas where comprehensive datasets are lacking. The generalizability of many recovery models also poses a challenge. These models are often tailored to specific damage scenarios or network configurations, limiting their utility in diverse or unforeseen hazard conditions. For instance, the phased recovery framework introduced by [16] demonstrates strong performance in urban environments where detailed demand data is available but struggles to adapt to rural or developing regions with less structured networks. Finally, resource allocation constraints are another significant limitation. Few recovery models explicitly address the dynamic redistribution of resources such as repair crews, equipment, or funding during the recovery process. [15] underscore this oversight, noting the potential for inefficiencies in resource allocation to hinder effective recovery efforts.

1.2. Contribution of this paper

The challenges of scalability, data dependency, generalizability, and resource allocation constraints in existing simulation-based recovery models highlight the need for further work in the field of resilience assessment and recovery planning in WDNs. Addressing these limitations requires models that not only simulate recovery dynamics but also adapt to diverse scenarios and resource constraints, while providing actionable insights for decision-makers.

To address these gaps, this paper introduces a post-earthquake resilience optimization model specifically tailored for WDNs. Its primary objective is to determine the optimal pipeline recovery sequence, aiming to prioritize the restoration of critical infrastructure components and ensuring a faster, more efficient return to full operational capacity. Building on an established resilience metric, this approach refines the assessment process to emphasize rapid system

recovery while maintaining adaptability and versatility across a broad range of scenarios. Unlike dynamic simulation approaches, which require meticulous fine-tuning of recovery strategies, this model eliminates the need to adjust parameters during optimization, thereby reducing execution time and complexity.

A distinguishing feature of the proposed work is its ability to capture system behavior under varying stress levels and resource availability. By simulating different combinations of these factors, the model produces characteristic curves. The curves that plot the chosen resilience metric against the recovery rate of the network, illustrate the WDNs' response to a complete range of hazardous scenarios. These curves provide a detailed perspective on how the system copes with disruptions, showcasing its capacity for resilience and adaptability in the face of changing conditions. For decision-makers, the characteristic curves can serve as a tool to effectively plan for and manage potential seismic events.

The key contributions of this paper can be summarized as follows:

1. Surrogate metric for resilience assessment: This paper employs a refined surrogate metric to evaluate the resilience of WDNs, providing a robust mechanism to enhance the understanding and quantification of network resilience.
2. Post-earthquake optimization model: It introduces an optimization model tailored for post-earthquake recovery of WDNs. It emphasizes swift and efficient recovery across the entire network by prioritizing critical components and optimizing recovery sequences.
3. Characteristic curves for system behavior: The framework generates detailed characteristic curves that capture WDN behavior under various hazard levels and resource availability conditions. These curves offer deep insights into system resilience, adaptability, and response patterns, serving as a practical tool for resilience analysis.
4. Resilience evaluation: The paper provides an evaluation of WDN resilience based on the generated characteristic curves. It facilitates informed decision-making, supporting resilience planning and enhancing of WDNs, in an effort to withstand and recover from disruptions.

By addressing existing gaps and introducing these novel contributions, the paper advances the state of the art in resilience assessment and recovery planning for WDNs, providing practical tools for disaster preparedness and management.

The remainder of this document is structured as follows: Section 2 provides a comprehensive description of the methodology followed in this work. Section 3 presents the numerical cases used to validate the proposed model, demonstrating its applicability and effectiveness in networks of different scale. Section 4 includes the discussion of the results. Finally, Section 5 presents the conclusions of the work.

2. Methodology

The primary goal of this study is to enhance the resilience of WDNs in the aftermath of seismic events, focusing specifically on the recovery of pipeline in-

frastructure. To achieve this, an optimization model is developed to prioritize the sequence in which damaged pipes are repaired, maximizing the network’s recovery efficiency. The outcome of this optimization process is extended through characteristic curves, which provide a detailed representation of the system’s performance under various stress levels and repair rate scenarios.

2.1. System modeling

This section describes how each component of the model is developed, establishing the foundation for accurately representing WDN performance under both normal and seismic conditions, along with its recovery process. Figure 1 depicts the methodology’s principal steps.

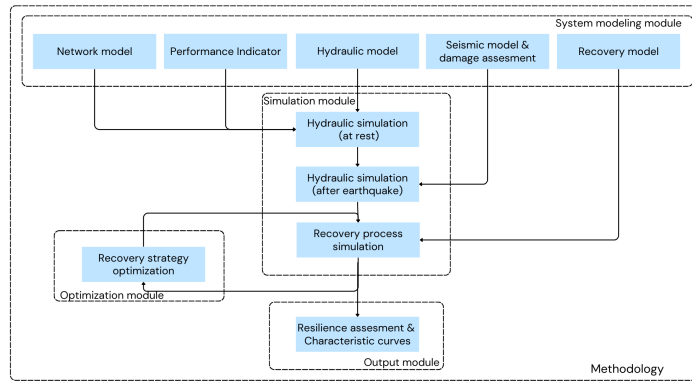


Figure 1: Methodology for the seismic resilience assessment of WDNs.

2.1.1. Network modeling

In this study, the WDN is modeled to include its primary components: nodes, pipes, pumps, and valves. The nodes, denoted by $n \in N$, includes junctions where water is consumed or distributed, as well as reservoirs and tanks. Reservoirs and tanks serve as storage elements with fixed water heads or varying water levels, depending on their role within the network. The pipes, denoted by $i \in P$, represent the physical conduits through which water flows, forming the backbone of the network’s connectivity and functionality. For the purposes of this analysis, nodes and pipes are considered the primary components, as they play the most critical roles in determining the hydraulic behavior and overall performance of the WDN. While pumps and valves are included in the model to ensure realistic simulation of network operations, they are excluded from the simulation of seismic damage and the subsequent recovery process. The study concentrates on the pipeline infrastructure within WDNs, under the assumption that other network components - such as pumps and tanks - either sustain minimal damage or can be quickly restored post-earthquake [5, 16, 20].

2.1.2. System performance indicator

The resilience of a WDN is evaluated by examining its performance across a time horizon sufficient to complete the restoration process following a disruptive event. To quantitatively assess the network’s performance, the study utilizes the Seismic Resilience Index (*SRI*), a metric that reflects the degree to which the network fulfills user demands under various operational conditions [16]. Thus, the resilience of WDNs is assessed through the levels of performance over time by calculating the area under the curve of the performance graph as shown in Figure 3. The overall performance of the WDN, is represented by the *SRI*, defined by [16] as:

$$SRI = \sum_{t=1}^T SDI(t) \quad (1)$$

where $SDI(t)$ is the Satisfaction Degree Index at each time step t . The Satisfaction Degree Index corresponds to the summation of the Node Satisfaction Degree of the nodes of the network, for a specific time-step and is expressed as follows:

$$SDI(t) = \sum_{n \in N} w_n \cdot NSD_n(t) \quad (2)$$

where w_n represents the weight associated with each node $n \in N$, reflecting its importance within the network. The Node Satisfaction Degree $NSD_n(t)$ for node n at time t is the level of satisfaction of a specific node for a specific time-step. It is calculated as the ratio between the hydraulic head that the network has at that particular node at that time-step against the hydraulic head that said node had before any disruptions. The $NSD_n(t)$ is given by the following formula:

$$NSD_n(t) = \min \left(\frac{H_n(t)}{H_n(0)}, 1 \right) \quad (3)$$

where, $H_n(t)$ is the hydraulic head at node n at time t , and $H_n(0)$ is the hydraulic head at the same node under normal pre-earthquake conditions. This ratio ensures that each node’s satisfaction is evaluated based on how closely the post-earthquake hydraulic head matches its normal operational head.

2.1.3. Hydraulic modeling

The recovery simulation begins with a detailed hydraulic simulation of the network in its normal, undisturbed state. This simulation establishes a baseline for the hydraulic head at each node, representing the pressure and water availability across the system. This baseline serves as a reference for evaluating the impacts of seismic events and the subsequent recovery process, providing a critical foundation for resilience analysis.

The study employs the Water Network Tool for Resilience (WNTR), a Python-based package specifically designed for modeling and analyzing the resilience of WDNs [22]. WNTR enables precise hydraulic calculations based on

well-established fluid mechanics principles, ensuring reliability and consistency with industry standards. The methodology follows the one used in EPANET 2, a widely used platform for hydraulic and water quality analysis, allowing for a robust simulation framework [23].

Key principles guide the simulation process, starting with the conservation of mass at each node. Additionally, the conservation of energy is applied throughout the network, modeling the effects of elevation changes, pipe friction, and pump contributions [23]. Water flow through the pipes is calculated using the Hazen-Williams equation [23], a widely accepted empirical formula for determining head loss due to friction.

$$h_f = k \cdot L \cdot \left(\frac{Q}{C}\right)^{1.852} \quad (4)$$

where h_f represents the head loss due to friction, measured in meters or feet, and k is a coefficient that depends on the pipe diameter and the unit system, which can be metric or imperial. The term L corresponds to the length of the pipe, measured in meters or feet, while Q denotes the volumetric flow rate, typically expressed in cubic meters per second or gallons per minute. Finally, C is the Hazen-Williams roughness coefficient, with higher values indicating smoother pipe interiors that result in lower frictional losses. In the context of this simulation, the Hazen-Williams formulation is adapted to handle negative flows, which occur when disruptions in the network, such as damaged pipes, cause water to flow in unintended directions.

To simulate network performance under low-pressure conditions, pressure-dependent analysis (*PDA*) is incorporated [24]. Unlike demand-driven models that assume constant water demands regardless of pressure, *PDA* adjusts demand based on the available pressure at each node according to Equation 5:

$$d(t) = d_{\max} \cdot \min\left(\frac{p(t)}{p_{\min}}, 1\right) \quad (5)$$

where $d(t)$ represents the actual demand at time t , and d_{\max} is the maximum demand the network is expected to satisfy. The term $p(t)$ denotes the available pressure at time t , while p_{\min} is the minimum pressure threshold required for full demand satisfaction. This approach is particularly important for post-damage scenarios, where reduced pressures can significantly impact the network's ability to meet user demands.

2.1.4. Seismic modeling and damage assessment

The next step in the model involves creating the disaster scenario and evaluating its impact on the WDN. This process begins with simulating a seismic event, which is defined by the earthquake's magnitude and the geographic location of its epicenter. The seismic intensity at different locations within the WDN is determined by calculating the peak ground acceleration (*PGA*) and peak ground velocity (*PGV*) based on the attenuation model selected, as functions of the distance from the epicenter.

To assess the damage caused by the seismic event, fragility curves are employed following the methodology outlined by [25]. Fragility curves provide a probabilistic representation of the likelihood that a pipeline will reach or exceed a specific damage state under given seismic conditions. In this analysis, the fragility curves are parameterized by the pipe repair rate and the pipe length. They define the probability of damage as a function of seismic intensity, incorporating empirical and analytical data on pipeline performance during earthquakes. Mathematically, the fragility curve for a pipeline is expressed as a cumulative distribution function (*CDF*), which relates the probability of exceeding a damage state ($P(D > d|IM)$) to the seismic intensity measure IM , such as PGA or PGV . The *CDF* is given by:

$$P(D > d|IM) = \Phi \left(\frac{\ln(IM) - \ln(IM_d)}{\beta_d} \right) \quad (6)$$

where Φ is the standard normal cumulative distribution function, IM_d is the median seismic intensity at which the pipeline is expected to reach the damage state d , and β_d is the logarithmic standard deviation, representing the variability in the damage threshold. These parameters are typically derived from empirical data and prior studies of pipeline performance under seismic loading [25].

For the purposes of this analysis, two distinct damage states are considered: "No Damage" and "Damage." The "No Damage" state represents pipes that remain fully functional, while the "Damage" state corresponds to pipes that are completely impaired along their entire length, rendering them unable to carry water flow. To simplify the modeling process, minor damages and leaks are excluded from consideration, focusing solely on major failures that significantly disrupt network functionality. The likelihood of each pipe's damage state is determined by sampling from the fragility curve using an exponential distribution, which is well-suited for modeling the stochastic nature of seismic damage [25, 26]. For a pipe with length L and repair rate λ , the probability density function *PDF* of damage over the length of the pipe can be expressed as:

$$P(\text{Damage}) = \lambda \cdot e^{-\lambda \cdot L} \quad (7)$$

Here, λ represents the repair rate, which is influenced by the seismic intensity and pipe properties, while L is the pipe length. Pipes that are sampled as undamaged retain their full functionality. Conversely, pipes classified as damaged are considered completely inoperative and are removed from the hydraulic model. This means that the damaged pipes are treated as closed, and water flow is redirected around the impaired sections. This assumption was considered in order to simplify the repair process, without having to consider different ways of addressing minor or major damages for the pipes. This reconfiguration alters the network's hydraulic behavior, introducing new constraints and potentially increasing head losses in alternative paths.

With the network now in its post-damage state, a hydraulic simulation is performed to calculate the updated hydraulic head at each node, reflecting the immediate impact of the earthquake. This simulation adheres to the principles

of conservation of mass and energy described in the earlier section, ensuring that the recalculated flows and pressures accurately represent the disrupted state of the network. The post-damage simulation captures the *SDI*, providing a quantitative basis for evaluating the network’s degraded performance.

2.1.5. Recovery modeling

The recovery process for the WDN begins immediately following the seismic event which is designated as day 0 in the simulation. This period marks the start of a structured and systematic effort to restore the damaged network, with repairs continuing over T days, the total recovery time required to fully repair the network under the specific scenario of the earthquake magnitude and the repair rate of the available crews. By definition, the recovery time T cannot exceed the maximum recovery time T_{\max} , which is determined as the number of days needed to restore full functionality to the network, under the most intense scenario of the highest magnitude and the lowest available repair rate.

The recovery process relies on the recovery sequence, denoted as \mathbf{X} , which specifies the order in which the damaged pipes will be repaired and is the product of the optimization model. Mathematically, \mathbf{X} is represented as a one-dimensional vector of length D , where D is the number of damaged pipes and P is the total number of pipes in the network, such that $D \leq P$. The sequence $\mathbf{X} = [x_1, x_2, \dots, x_D]$ defines the repair order, with x_i representing the position of the i -th damaged pipe in the sequence.

Repair crews are assumed to have a fixed daily repair capability, referred to as the repair rate, which is measured in meters of pipeline that can be repaired per day. This repair rate, denoted by R , is a critical parameter in the simulation, reflecting the resources of the repair effort. The crews are considered fully equipped and ready to begin repairs immediately following the seismic event. Importantly, repairs are modeled as non-preemptive; once a crew starts repairing a pipe, they must complete the repair of that pipe before moving to the next one in the sequence.

The recovery sequence \mathbf{X} is transformed from a one dimensional vector into a matrix $\bar{\mathbf{X}}$ for the purposes of the simulation. This matrix tracks the repair status of each pipe over time, with dimensions $P \times (T_{\max}/\Delta t)$, where Δt is the time-step that is chosen to divide the recovery period. In this case the time-step selected corresponds to one day, therefore $\Delta t = 1$. The above transformation is necessary, since the recovery sequence \mathbf{X} contains only the order with which every damaged pipe is to be repaired. However, the time that is necessary for every repair is an important aspect of the recovery process. The matrix $\bar{\mathbf{X}}$ translates the recovery sequence \mathbf{X} into the damaged state of every damaged pipe for every day of the recovery process. Each entry \bar{X}_{it} indicates the proportion of pipe i that remains damaged at day t . Initially, $\bar{X}_{it} = 1$ for all damaged pipes:

$$\bar{X}_{it} = 1 \quad \forall t \in \{1, 2, \dots, T_{\max}\}.$$

The repair process unfolds iteratively, with repair crews addressing the pipes sequentially based on the order defined in \mathbf{X} . At the beginning of each day, the

available repair capability is initialized to the predefined repair rate R . The crew then assesses the remaining length of the pipe currently under repair, denoted as J_i , which represents the length of pipe i that has yet to be repaired. If the remaining length is less than or equal to the available repair rate, the pipe is fully repaired that day. This means it is marked as fully functional, and the remaining repair rate is reduced by the length of the repaired pipe. The matrix $\bar{\mathbf{X}}$ is updated to reflect that $\bar{X}_{it} = 0$, indicating that no further repairs are required for this pipe.

For pipes where the remaining length exceeds the daily repair rate, only a portion of the pipe is repaired, equivalent to said available repair rate. The remaining length is reduced accordingly, and \bar{X}_{it} is updated to reflect the proportion of the pipe still requiring repair. In this scenario, the repair rate for the day is depleted to zero, and the repair of the pipe continues into the next day. The process iterates through the recovery sequence until either the daily repair rate is exhausted or all pipes in the sequence have been addressed. \bar{X}_{it} offers a collective view of the recovery process for every time-step of its duration.

At the end of each day, a hydraulic simulation is conducted to update the state of the WDN. This recalculates the hydraulic head at each node, incorporating the restored functionality of the repaired pipes. The Satisfaction Degree Index SDI is recalculated after each simulation, providing a quantifiable measure of the network’s improving functionality as repairs progress.

This process continues until all damaged pipes have been fully repaired or the recovery period concludes. By iteratively updating the repair status matrix $\bar{\mathbf{X}}$ and recalculating network performance metrics, the model provides a detailed and realistic representation of the post-disaster recovery effort. This structured approach ensures that repair resources are systematically allocated, enabling an efficient and effective restoration of the WDN.

2.2. Recovery strategy optimization

This section presents the mathematical formulation of the proposed optimization model, which determines the most effective recovery strategy for a damaged WDN. The primary objective is to maximize network resilience by optimizing the sequence in which damaged pipelines are repaired.

The recovery strategy is represented by the vector $\mathbf{X} = [x_1, x_2, \dots, x_D]$, where each element x_i denotes the repair order of the i -th damaged pipe. Each variable x_i is an integer constrained within the range $[0, D]$, with D being the total number of damaged pipes. The objective of the optimization model is to maximize network resilience by minimizing the negative of the time-weighted SDI over the recovery period T . The objective function is formulated as:

$$\min_{\mathbf{X}} - \sum_{t=1}^T \frac{SDI_t(\mathbf{X})}{t} \quad (8)$$

This formulation penalizes slower recovery strategies by weighting earlier improvements in the network’s performance more heavily. Rapid recovery is a main characteristic of better resilience, as delays in functionality restoration

have negative impacts on consumers and overall network functionality. The inclusion of the time factor t ensures that the optimization process prioritizes strategies that achieve restoration efficiently. As illustrated in Figure 2, faster recovery curves demonstrate higher resilience, as reflected by the area under the curve. The time-penalized objective function promotes strategies that achieve restoration in the shortest possible time.

The optimization problem is subject to several constraints ensuring practical and feasible recovery strategies:

Order constraint: The order in which the damaged pipes are repaired must be feasible and remain within the total number of damaged pipes:

$$0 \leq x_i \leq D, \quad \forall i \in \mathcal{D} \quad (9)$$

This ensures repair actions are applied only to damaged pipes within the network, as represented by the set D . It prevents assigning repair actions to undamaged pipes and guarantees that the repair process is directed only towards pipes that require intervention.

Permutation constraint: Each damaged pipe must be repaired exactly once, and the order of repairs must be unique:

$$x_i \neq x_j, \quad \forall i \neq j, \quad i, j \in \mathcal{D} \quad (10)$$

This constraint enforces that no two pipes can be repaired simultaneously or receive duplicate repair assignments. In practical terms, it ensures that the repair crew attends to each pipe once and only once. This constraint is essential to avoid any overlap or redundancy in the repair sequence, which would otherwise compromise the efficiency of the recovery strategy.

Head constraints: The hydraulic head at each node in the network must remain within a predefined range during the recovery process. These constraints ensure the network operates within safe and acceptable performance limits:

$$H_{\min} \leq H_{n,t}(X) \leq H_{\max}, \quad \forall n \in \mathcal{N}, \forall t \in \{1, \dots, T\} \quad (11)$$

Additionally, the minimum head H_{\min} must be non-negative to ensure a physically feasible operation:

$$H_{\min} \geq 0 \quad (12)$$

2.3. Resilience assessment & Characteristic curves

To evaluate the broader performance during the recovery phase, the near-optimal recovery strategy is analyzed under diverse scenarios, including varying earthquake intensities and different repair rates for multiple repair crews. For each scenario, the calculated *SRI* values are used to generate characteristic curves, which visually represent the relationship between network resilience and recovery rates.

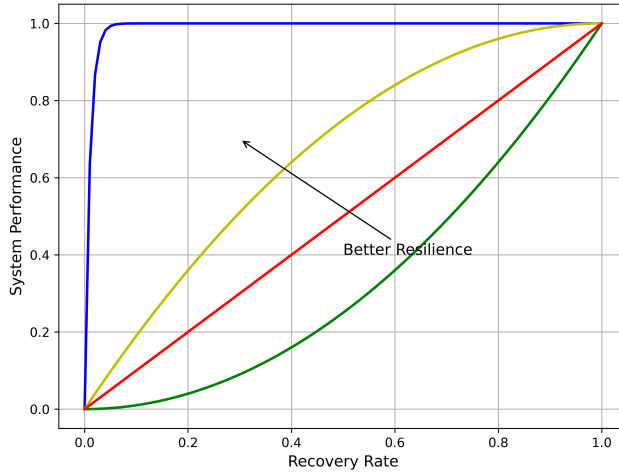


Figure 2: Example of characteristic curves depicting the system’s recovery capacity.

Optimal recovery behavior is characterized by a network that achieves maximum performance with the lowest repair rate, as shown in Figure 2. The construction of characteristic curves involves two components: the performance matrix for the selected resilience metric and the recovery rate. The performance matrix is derived from the *SDI* values, which capture the WDNs performance at every time-step t as demonstrated in Equation 2. These values are computed based on the optimal repair sequence for various earthquake intensity levels and represent the dynamic state of the network during recovery. The matrix is structured such that each row corresponds to a specific damage level l and each column to a discrete time-step t , forming a two-dimensional array of performance metrics. The dimensions of the matrix are determined by $m \subseteq \mathcal{M}$, the number of damage levels M considered in the analysis, and T_{\max} , the maximum recovery time required under the most severe scenario.

The average performance of the network for a given hazard level is calculated by averaging the *SDI* values over T_{\max} , the total time required to fully recover the network under the worst-case conditions. This approach ensures that the performance matrix accounts for the network’s performance at its most vulnerable state, providing a robust foundation for evaluating resilience across different scenarios. Mathematically, the performance matrix is represented as:

$$SDI_{m,t} = \begin{bmatrix} SDI(1,1) & SDI(1,2) & \dots & SDI(1,T_{\max}) \\ SDI(2,1) & SDI(2,2) & \dots & SDI(2,T_{\max}) \\ \vdots & \vdots & \ddots & \vdots \\ SDI(M,1) & SDI(M,2) & \dots & SDI(M,T_{\max}) \end{bmatrix} \quad (13)$$

This formulation ensures that the performance matrix captures the temporal

recovery dynamics of the WDN for various hazard levels, forming the basis for constructing characteristic curves and evaluating resilience metrics.

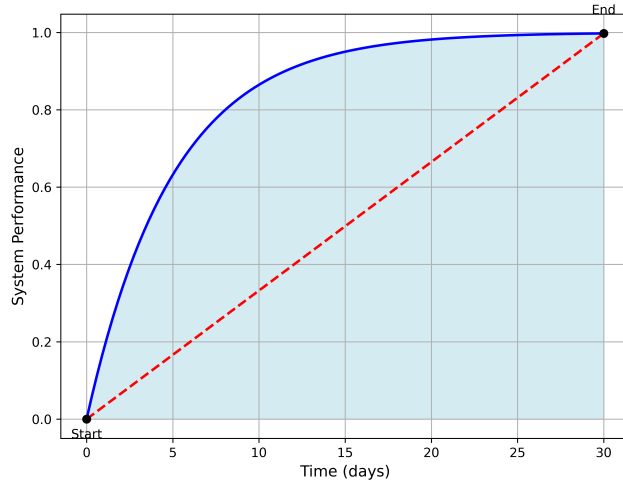


Figure 3: Resilience curve illustrating the repair rate as the secant of the SDI curve.

In parallel, the recovery rate is defined as the average hydraulic head that is regained by the whole network over the total of the recovery period and is measured in m/day . It is calculated as the secant of the SDI curve for each combination of damage level and repair rate, providing a quantitative measure of the efficiency of recovery efforts. The recovery rate is particularly valuable for comparing scenarios with different resource constraints and damage intensities, offering insights into how resource allocation impacts the pace of recovery. Figure 3 illustrates an example of the resilience curve with a secant line representing the recovery rate.

The characteristic curves generated from this analysis are instrumental for evaluating the WDN’s performance under diverse stress scenarios. They provide decision-makers with a clear understanding of whether the available resources are sufficient to address specific levels of network damage and allow for the identification of critical thresholds where additional resources may significantly enhance recovery efficiency. Furthermore, the curves underscore the importance of proactive planning and preparedness, as they highlight the relationship between resilience and resource allocation across different damage levels.

3. Application cases

To illustrate the applicability of the proposed model, this section presents its implementation across two distinct case studies involving WDNs. The first

case study focuses on a small, standardized benchmark network commonly used for evaluating WDN models. This network provides a controlled environment to validate the core functionality of the proposed model. The second case involves a scalable network that approximates the characteristics of a small, real-world water distribution system.

3.1. Case 1

3.1.1. Case description

The first case study is a modified version of Network 1 from the EPANET example set, provided by the US Environmental Protection Agency (EPA).

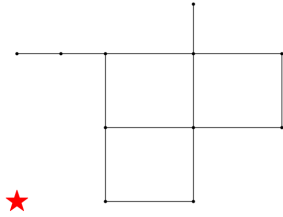


Figure 4: Illustration of Network 1 from the EPANET example set and the location of the epicenter of the earthquake.

Pipe IDs	Length (km)
"10"	3.2
"11"	0.8
"12"	1.6
"21"	1.6
"22"	0.7
"31"	0.6
"110"	0.6
"111"	2.1
"112"	0.8
"113"	3.0
"121"	3.0
"122"	0.9

Table 1: Pipe names and corresponding lengths for Network 1.

This network comprises 12 pipes, 9 junctions, 1 pump, 1 tank, and 1 reservoir, as illustrated in Figure 4. The junctions' demands are modeled to follow a 24-hour demand pattern, reflecting realistic variations in water usage over time. To enhance the applicability of the case study, the pipes' lengths were modified slightly from their original values in Network 1. These changes were made to introduce variability in pipe lengths, as the original configuration included groups of pipes of uniform length. This adjustment prevents the optimization algorithm from converging prematurely on solutions influenced by uniform pipe lengths, ensuring a more realistic evaluation. The total length of the network's 12 pipes amounts to 19 km, while the length of every pipe can be seen in Table 1.

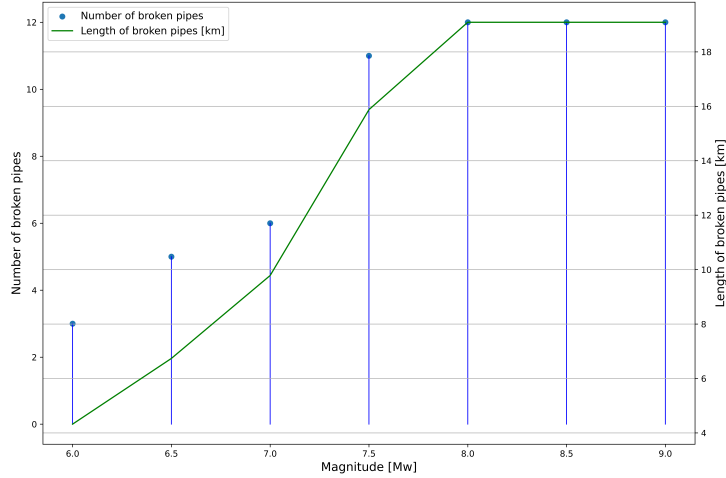


Figure 5: Kilometers of broken pipes and number of broken pipes versus earthquake magnitudes for Network 1.

The epicenter of the simulated earthquake is located at the bottom left corner of the network, as can be seen in Figure 4. Earthquake magnitudes ranging from 6.0 Mw to 9.0 Mw were considered to assess their impact. The relationship between earthquake magnitudes and the extent of damage is depicted in Figure 5.

3.1.2. Optimal recovery strategy

As was discussed in Section 2, the recovery strategy is generated by a GA. This section presents the results for one severe scenario, where the earthquake magnitude reaches 9.0 Mw and there is available only one repair crew with a daily repair rate limited to 25 m/day . For this case, we compare the optimal repair strategy, produced by the GA, to two baseline strategies for prioritizing broken pipes. The first is based on average demand where the priority of the pipes is given in descending order of the average demand for their start and end nodes. The second is based on the average hydraulic head. According to this one, pipes are ranked by the average hydraulic head at their start and end nodes, giving priority to those that potentially carry higher pressure.

Figure 6 displays the SDI trajectories for all three approaches. Each discrete step in the optimal curve marks the completion of a pipeline repair. Notably, the optimal (red) strategy rises more quickly and achieves a final SRI of 0.831, surpassing both the head-based strategy (blue, 0.536) and the demand-based strategy (yellow, 0.255). Although perfect resilience, i.e., $SRI = 1$, was not achievable for the optimal strategy, due to the extended recovery period, 90% of the SDI is restored within the first year and 9 out of 12 pipes were fully repaired during this time.

The recovery curve for the optimal sequence, highlights a rapid initial restoration, followed by a gradual ascent to full functionality as repairs progressed.

This pattern reflects the prioritization of critical pipes during the early recovery phases, with subsequent efforts focused on restoring the network’s remaining capacity. In contrast, both of the fixed strategies under-perform. The priority for pipes with the highest values of hydraulic head and demand accordingly, results in an inefficient behavior. The demand based approach, does not make use of the connectivity of the network. It focuses on repairs for pipes that once repaired, seem to not contribute to the reinstating of the flow and the accumulation of high SDI . That is evident from the trajectory of the SDI curve, where the recovery of almost all the pipes needs to be completed in order for the final repairs to restore the flow and increase the SDI value close to 1.0. The head based approach, produces a curve that is more similar to the optimal one. That is expected since the hydraulic head is the driving factor for the prioritization of the pipe. However, it still fails to exploit the redundancy of the network and aim to repair the most important pipes according to the highest SDI . Instead, it targets pipes with the same high value of hydraulic head, even though they are not all necessary for the restoration of flow in the network. This results to a slower restoration of the SDI and a smaller resilience for the network’s recovery process, reflected in a smaller value of the SRI .

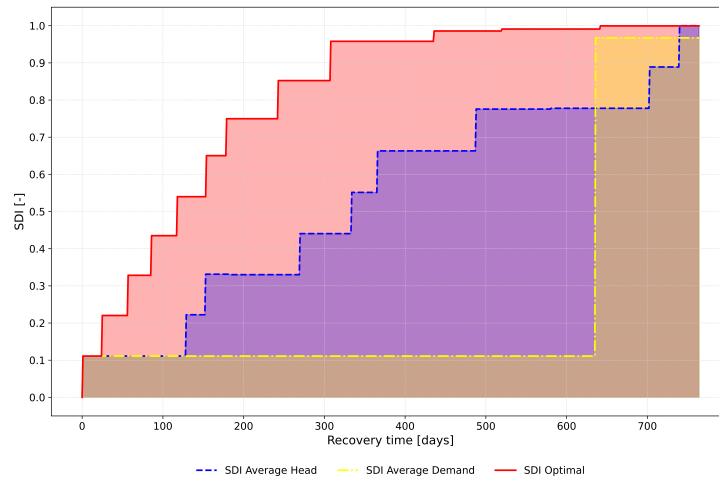


Figure 6: SDI curve for network 1 for the optimal recovery sequence and for the fixed strategies.

The results of the GA’s search process are provided by the box-plot in Figure 7, which illustrates the progression of solution quality across generations. During the early generations, the interquartile ranges were wide, reflecting significant exploration by the algorithm. This variability ensured that the GA explored a diverse set of potential recovery sequences. By generation 14, the interquartile range had narrowed considerably, indicating that the population was converging toward high-performing solutions. Full convergence was achieved in generation 17, with minimal variability in fitness values thereafter.

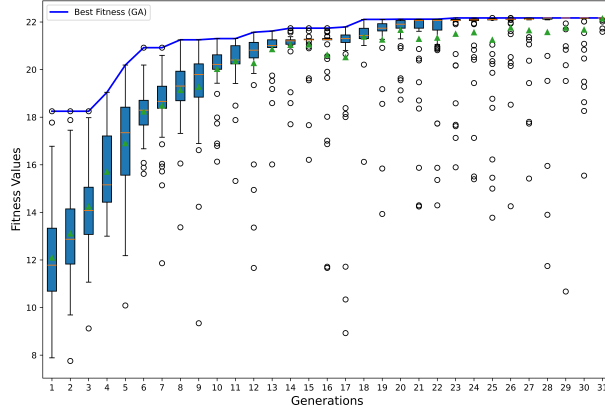


Figure 7: Box-plot of the results of the GA search for Network 1.

The presence of outliers in later generations highlights the algorithm’s ongoing exploratory processes, even after convergence. These outliers represent alternative solutions explored by the GA, which helps maintain diversity within the population. However, their limited impact on the overall fitness values suggests that the convergence to the optimal solution is robust. The algorithm’s ability to balance exploration and exploitation reinforces confidence in its performance.

3.1.3. Characteristic curves

This section presents the characteristic curves for Network 1, illustrating the restorative behavior of the network under varying earthquake magnitudes and different levels of available repair resources. These curves provide a comprehensive representation of the system’s performance as it responds to stress scenarios, independent of the specific earthquake magnitudes and recovery resources.

Figure 8 depicts the *SRI* achieved by the network during the repair process, based on the optimal recovery sequence. The results are presented as a function of recovery rate, defined as the average restoration rate from the start to the completion of the recovery process. Each distinct line in the graph corresponds to a specific number of repair crews, with repair rates ranging linearly from 25 *m/day* (1 crew) to 150 *m/day* (6 crews). Points along each line represent the ascending magnitude levels from 6.0 *Mw* on the top of every curve to 9.0 *Mw* on the bottom.

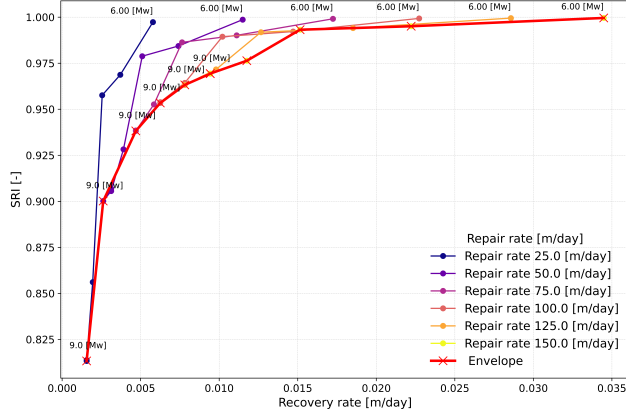


Figure 8: Characteristic curves of SRI as a function of recovery rate for varying repair rates in Network 1.

The graph reveals several trends. For low earthquake magnitudes, such as 6.0 Mw , the network is capable of achieving full recovery i.e., $SRI = 1$, regardless of the repair rate. However, for higher earthquake magnitudes, such as 9.0 Mw , the resilience of the system diminishes and is dependent on the repair resources. At a repair rate of 25 m/day , the network is unable to achieve a resilience metric of 1.0 with the SRI reaching only 0.810, due to the extended recovery time. As the repair rate increases, the SRI value increases with the highest value achievable being 0.970 for the maximum available repair rate of 150 m/day . This indicates that for severe damage scenarios, even the maximum available repair resources are insufficient to fully guarantee the maximum desirable level for the network's resilience.

In terms of the recovery rate of the network, it is interesting to note that for small magnitudes we can observe that an increase in available repair crews, directly translates to a proportional increase in recovery rate. This demonstrates a linear relationship between repair resources and recovery efficiency. Conversely, that is not the case with increasing magnitudes. As the damage severity becomes greater, the recovery rate does not scale linearly with the repair rate. For 6.0 Mw , the recovery rate increases proportionally to the repair rate, however, for 9.0 Mw , the increase in recovery rate is only about one-third of the increase in repair rate. This diminishing return highlights the complexity of the network's performance as the extent of damage becomes more severe. In the cases of greater damage extent, the recovery process needs to target several pipes before a sufficient amount of them has been restored. By creating a pathway of critical pipes that will serve the network and provide adequate pressure to the consumers, the restoration process continues until the full repair of all the pipes of the network. This process is reflected in slower recovery rates.

At lower repair rates (e.g., 25 m/day), the network recovers slowly, with the

recovery rate close to 0.005 m/day , emphasizing the need for increased resources to mitigate prolonged disruptions. With increased repair rates (e.g., 150 m/day), near-total recovery can be achieved in shorter time-frames and greater recovery rates. However, it is necessary to examine the cost of the investment against the benefit of recovery in terms of time and functionality. According to the characteristic curves, for greater damage levels, the increase in repair resources is not guaranteeing a similar extent of increase for the recovery rate or the resilience metric of the network. That would mean that a different deployment of resources is perhaps necessary to address the needs of the network.

Figure 9 shifts focus to the influence of earthquake magnitudes on recovery dynamics. It examines SRI as a function of recovery rate for seismic intensities ranging from 6.0 Mw to 9.0 Mw . The graph highlights how initial damage levels, dictated by earthquake magnitude, impact the recovery trajectory.

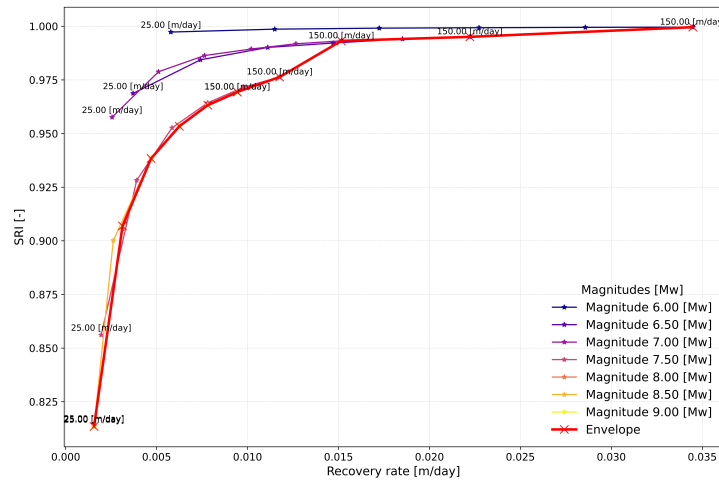


Figure 9: Characteristic curves of SRI as a function of recovery rate for varying earthquake magnitudes in Network 1.

For lower earthquake magnitudes, such as 6.0 Mw , the network experiences minimal initial damage, reflected in higher starting SRI values. It is interesting to note that the different magnitudes can be clustered into three separate groups based on the network's behavior. For magnitude 6.0 Mw , the network is practically unbothered. Magnitudes until 7.0 Mw result in small damages, where the SRI is close to 0.95 for one crew, while being able to recover quite easily, making evident that 3 crews are more than enough. However, for magnitudes greater than 7.5 Mw , the extent of the damage becomes important enough, so that the available resources are not able to fully restore the network and the proportionality of their increase is not reflected in the recovery rate.

The recovery curves for higher earthquake magnitudes display a steeper slope, signifying slower progress in restoration despite an increase in repair resources. Again, this highlights the significance of the initial damage, since one

might otherwise expect a linear correlation between resource availability and recovery rate.

3.2. Case 2

3.2.1. Case description

The network selected for the second case study is Network 3, in the EPANET example set, provided by the US Environmental Protection Agency (EPA).

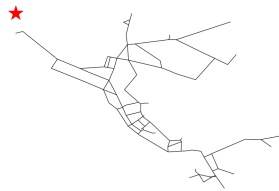


Figure 10: Illustration of Network 3 from the EPANET example set and the location of the epicenter of the earthquake.

Pipe IDs	Length (km)
"20"	0.03
"40"	0.03
"50"	0.03
"60"	0.3
"101"	4.3
"103"	0.4
"105"	0.7
"109"	1.2
"111"	0.6
...	...
"330"	3.0
"333"	0.9

Table 2: Pipe names and corresponding lengths for Network 3.

The EPANET Network 3 is based on the North Marin Water District (NMWD) in Novato, CA. NMWD serves a population of around 64,000 people over an area of about 100 mi². A significantly larger and more complex system with 118 pipes, 92 nodes, 2 pumping stations, 3 tanks, and 2 constant head reservoirs, illustrated in Figure 10. The network was used as part of a water quality study of the system [27]. The demand pattern of this network follows a 24-hour pattern like in the Section 3.1, while the total length of the network's 118 pipes amounts to 150 km. Table 2 presents a fraction of the lengths of the network's pipes, while the full table is available in the Appendix.

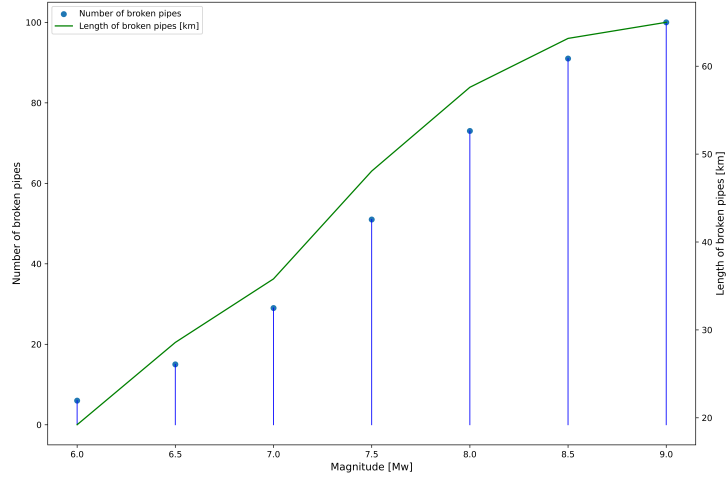


Figure 11: Kilometers of broken pipes and number of broken pipes versus earthquake magnitudes for Network 3.

The earthquake epicenter is located close to the top left corner of the network. Earthquake magnitudes ranging from 6.0 M_w to 9.0 M_w were considered to assess their impact, resulting in varying numbers of broken pipes across the network, as can be seen in Figure 11.

3.2.2. Optimal recovery strategy

The discussion initially focuses on the most vulnerable state of the network: a scenario with the highest earthquake magnitude and only one available repair crew. Figure 12 presents the recovery of hydraulic performance, measured using the SDI , comparing the near - optimal recovery sequence, with the two baseline strategies. Similarly to the first numerical case, the near - optimal strategy outperforms both of the baselines. The SRI for this scenario is calculated to be 0.698, reflecting the network's reduced resilience under such limited repair resources. Still, an improvement over the value of 0.372 for the average head based strategy and the 0.272 for the average demand based strategy. The optimal strategy seems to offer the fastest initial restoration of critical pipes, resulting in an early jump for the SDI values in Figure 12. Overall, the SDI curve has a convex-looking appearance, prioritizing pipes that have the biggest influence on the metric, as was expected from the definition of the optimization problem. However, that is not the case for the other two baseline strategies. The blue curve, the average head based strategy, spends the first 800 days repairing pipes with small impacts on the SDI and then its slope increases, exhibiting an undesirable performance in terms of the resilience, as it is not promote high early recovery. A similar behavior can be observed in the average demand based strategy, where for almost half of the recovery time the SDI remains close to zero and then, after the reparation of a lot of less critical pipes, there is enough flow in the network to increase the SDI levels.

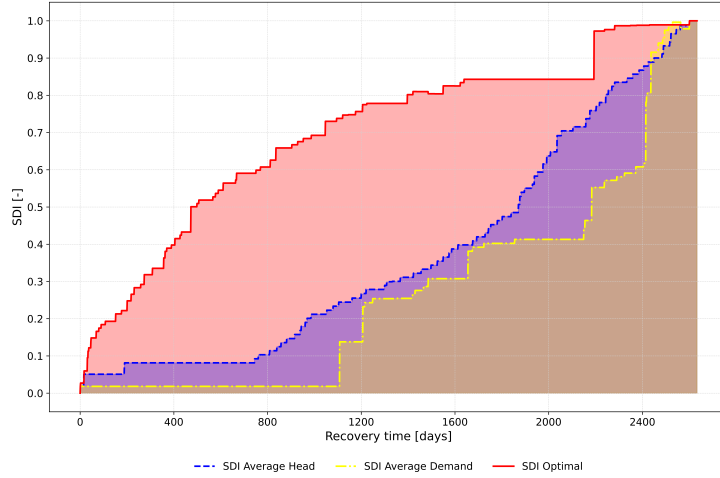


Figure 12: Recovery curve of Network 3 with one crew (25 m/day repair rate).

The complexity of Network 3 is evident in the graph, which shows a more intricate recovery curve compared to the smaller network in Section 3.1. The inefficiency of having only one repair crew is also apparent, as full recovery takes nearly 2500 days (approximately 6.5 years). Such a prolonged recovery period would be unacceptable in real-world scenarios. In this scenario, the network undergoes continuous repair for approximately 3.5 years, during which the *SDI* steadily improves, reaching 80% of full recovery. Following this phase, there is a plateau lasting more than one year, during which the *SDI* remains unchanged. That is attributed to the repair process of a single pipe with a length of 14 km. At a repair rate of 25 *m/day*, this pipe alone requires more than 500 days to repair, explaining the stagnation in the *SDI* during this period. Similar plateaus are observed in the two baseline strategies, however they are evident in different times, highlighting the difference in prioritization for the pipe.

Given the slow recovery associated with one crew, two more cases are chosen to be presented. Both of these cases have magnitude 9.0 *Mw* while the repair rate of the first is 75 *m/day* corresponding to 3 crews and the second has repair rate of 150 *m/day*, corresponding to 6 crews. For the case of 3 repair crews and a repair rate of 75 *m/day*, the near-optimal strategy of the GA had an *SRI* equal to 0.896, while the average head strategy an *SRI* of 0.791 and the average demand strategy an *SRI* of 0.757. The total recovery period concluded within 3 years. The results are shown in Figure 13.

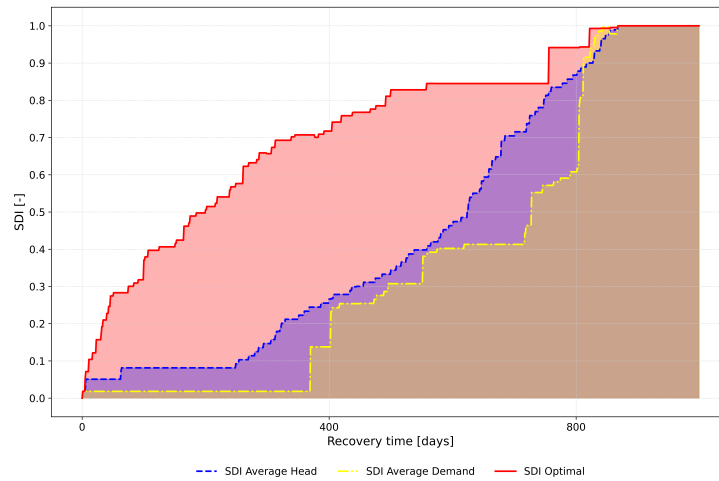


Figure 13: Recovery curve of Network 3 with three crews (repair rate of 75 *m/day*).

Figure 14 shows the results for 6 repair crews and a repair rate of 150 *m/day*, the near-optimal strategy of the GA had an *SRI* equal to 0.948, while the average head strategy an *SRI* of 0.895 and the average demand strategy an *SRI* of 0.879.

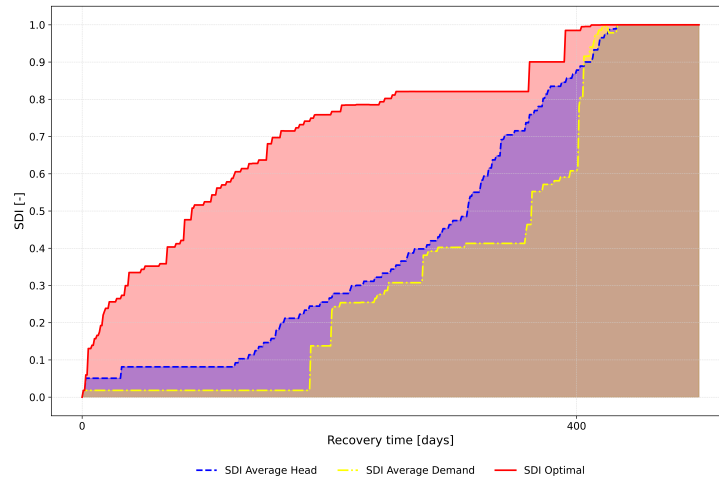


Figure 14: Recovery curve of Network 3 with three crews (repair rate of 150 *m/day*).

The performance of the near - optimal solution and that of the baseline strategies for the two additional cases, remains relatively the same, with small deviations. The importance of the increased repair rate is reflected on the recovery time. For a crew of 6 people, the recovery is complete in under 500 days compared to 2500 for one crew. That means that there is an almost

proportional decrease of recovery time with the increase of recovery resources. However, in terms of the resilience metric, there was only an increase of around one quarter.

The results of the GA for the scenario of magnitude 9.0 Mw and repair rate 25 m/day are provided by the box plot shown in Figure 15. The plot shows that the presence of outliers is more pronounced in this case compared to Section 3.1. While the results indicate that the algorithm is approaching the optimal solution, the variability and persistence of outliers suggest that additional runs are necessary to refine the solution and ensure convergence.

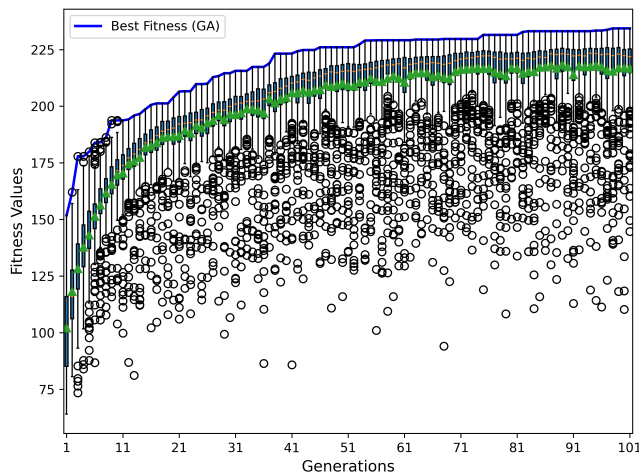


Figure 15: Box plot of GA training for Network 3 with one crew (repair rate of 25 m/day).

The GA results for Network 3 demonstrate the challenges posed by the increased scale and complexity of the network. While the algorithm successfully identifies high-performing recovery sequences, the computational demands and slower convergence highlight the need for further optimization and additional computational resources.

3.2.3. Characteristic curves

In this section, the characteristic curves for Network 3 are presented, following the same approach as in the first numerical case. While the general trends already observed hold for this larger and more complex network, Network 3 introduces additional challenges due to its scale and intricacy.

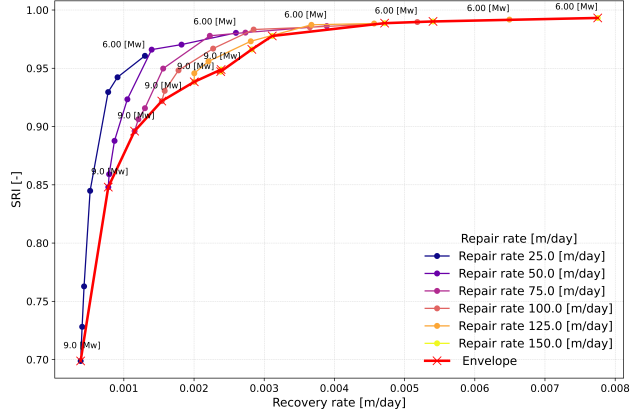


Figure 16: Characteristic curves of SRI as a function of recovery rate for varying repair rates in Network 3.

Figure 16 illustrates the relationship between the SRI and the recovery rate for different repair capacities in Network 3. Similar to Section 3.1, each line represents a specific number of repair crews, with repair rates ranging from 25 m/day (1 crew) to 150 m/day (6 crews). The points along the lines correspond to varying earthquake magnitudes starting from magnitude 6.0 Mw to 9.0 Mw .

Several key differences emerge due to the increased complexity of Network 3. Unlike the smaller network in the first numerical case, where a magnitude 6.0 Mw earthquake had no noticeable impact on the network's resilience at lower repair rates, Network 3 experiences a drop in SRI even at the lowest magnitude. This reflects more intricate inter-dependencies within the network, which make it more sensitive to seismic events. At higher magnitudes, such as 9.0 Mw , the SRI fails to reach 1.0, even with the maximum number of repair crews. For the lowest magnitude, 6.0 Mw , the network also cannot fully recover, achieve $SRI = 1$ with the available resources, highlighting the need for greater investments in repair capacities to address the larger damage scope of a complex network. The trend of proportional increase of the recovery rate with an increase of the repair rate for earthquakes of small magnitudes is also evident here. However, the nominal recovery rates achieved in Network 3 are lower, reflecting the challenges posed by its scale and complexity. Network 3 is larger and more complex than Network 1 and that difference is reflected in the characteristic curves of Figure 16.

Figure 17 shifts the focus to the effect of earthquake magnitudes on the recovery dynamics of Network 3. The graph examines the SRI as a function of recovery rate for seismic intensities ranging from 6.0 Mw to 9.0 Mw .

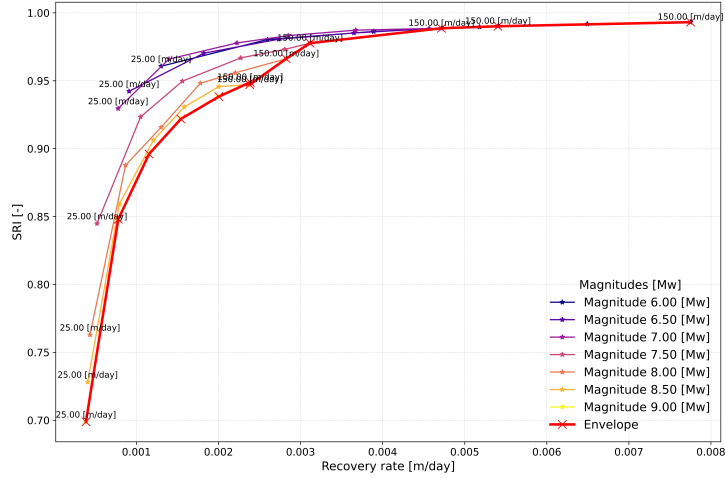


Figure 17: Characteristic curves of SRI as a function of recovery rate for varying earthquake magnitudes in Network 3.

The trends observed in the first case are generally consistent, but Network 3 exhibits some notable differences due to its scale. Even for lower magnitudes, such as 6.0 Mw , the SRI begins at a lower value, particularly at small recovery rates. This contrasts with the first case, where the SRI remained unaffected at lower magnitudes. The added complexity and interconnections in Network 3 makes it more vulnerable, even to moderate seismic stresses. At higher magnitudes, such as 9.0 Mw , the network’s initial SRI is significantly reduced, and the recovery process is slower. Even with the highest repair rates, the network struggles to achieve full recovery. This highlights the increased resource demands of larger systems and the limitations of existing repair rates. The diminishing gap between SRI curves for different magnitudes as recovery rates increase underscores the importance of scaling repair resources proportionally to the severity of seismic events. Additionally, the slower recovery rates observed in Network 3 emphasize the challenges of achieving similar levels of efficiency as seen in smaller networks.

4. Discussion

This study aims to develop an optimization model to enhance the resilience of WDNs after seismic events. The focus was on determining optimal repair sequences for damaged pipelines, maximizing recovery efficiency. By combining recovery simulations with characteristic curves, the proposed work offers a comprehensive approach to enhance the resilience of WDNs.

The optimal repair sequence generated by the GA consistently achieves higher SRI values than the fixed strategies. Overall, the resilience curve of the optimal strategy performs better than the benchmark strategies, by prioritizing critical pipes and promoting faster initial recovery of the system. Moreover,

the optimal strategy maintains its positive performance for networks of different sizes, in contrast with the benchmark strategies which exhibit greater variability in their performance. The characteristic curves reflect the recovery properties of the network and provide valuable insights into the relationship between resource allocation, recovery rates, and resilience. They offer a visual representation of the achievable levels of resilience and recovery rate for different damage levels and available resources. The complexity of different networks is reflected in their shape, providing a possible classification tool for comparable networks.

The study’s findings align with existing research, emphasizing the importance of pipeline recovery optimization in enhancing WDN resilience and the utility of GA as a means of solving optimization problems. The integration of characteristic curves into the analysis represents a novel contribution. The characteristic curves offer a comprehensive view in the resilience of the system and provide a connection between the available resources, the initial damage levels and the recovery of the system. This study also provided new insights into the scalability challenges faced by larger networks, emphasizing the need for tailored recovery strategies. Contrary to earlier research and existing practice suggesting near-linear benefits from additional resources, our results—particularly in the more complex network—indicate a more nuanced reality. By interpreting the characteristic curves of the examined networks, it is evident that for greater damage severity, the increased resources while speeding recovery, they are not able to provide a comparable restoration process. While resource allocation remains crucial, simply adding more crews does not automatically yield proportional improvements; instead, optimal planning could be a solution to realize meaningful resilience gains.

Building on that consideration, the current model assumes that repair crews work serially on a single pipe at a time. While this simplification makes the model easier to implement and analyze, it does not leverage the potential benefits of deploying multiple crews simultaneously across different parts of the network. A more complex implementation that allows for parallel crew operations could significantly enhance the network’s recovery capacity. However, such an approach would increase the computational complexity and require more advanced optimization strategies to manage the coordination and prioritization of multiple repair teams effectively. The computational intensity of the GA is also poses limitations on the existing model, especially for larger networks. For the second case study, the computational demands required leveraging the Delft-Blue supercomputer at the Delft High Performance Computing Centre (DHPC) [28]. This reliance on high-performance computing highlights a key limitation of the approach when applied to expansive or highly interconnected networks. Balancing these complexities with practical applicability remains a challenge for future iterations of the model.

For asset managers and water authorities, the model offers a valuable tool for prioritizing pipeline repairs and optimizing resource allocation, enabling more efficient and effective recovery efforts. The introduction of characteristic curves provide significant advantages for the resilience analysis of WDNs. They can enable decision-makers to prepare and plan for desirable recovery outcomes. By

capturing the behavior of the networks, the curves facilitate strategic resource allocation, ensuring that investments are directed toward maximizing recovery efficiency. These curves also simplify complex recovery dynamics into actionable insights, helping asset managers, engineers, and policymakers make informed decisions.

Future work should aim to enhance the optimization model by incorporating dynamic resource allocation to reflect real-world constraints and variability in repair resources. Additionally, applying the model to more complicated and extensive networks would ensure its scalability and relevance to real-world applications, making it a valuable tool for large urban systems. The model could also be improved by assigning different weights to network nodes, reflecting the varying criticalities of system users such as hospitals, shelters, and industries, to better evaluate their impact on the *SRI*. The characteristic curves could be further developed by incorporating acceptable thresholds tailored to specific impacts of different hazard levels, enabling a more nuanced analysis of resilience. Expanding the scope of the work to address additional hazards beyond earthquakes, such as floods, wildfire, or man-made attacks, would increase its applicability. Finally, integrating an economic component to evaluate the costs associated with the resource allocations suggested by the characteristic curves would provide decision-makers with insights into the financial implications of various recovery strategies, ensuring both efficiency and cost-effectiveness.

5. Conclusions

This study introduces an optimization method for determining the most effective pipeline repair order, yielding significantly higher resilience indices compared to pre-existing fixed-priority strategies. It effectively maintains improved recovery outcomes regardless of network size, underscoring its capacity for broader application. Furthermore, the creation of characteristic curves offers a comprehensive perspective on system recovery by mapping the relationship between resource allocation, initial damage level and recovery aspects of the system. From a policy making standpoint, these curves can serve as a tool for resilience network classification and optimal investment decisions, especially in cases of significant initial damage where the connection between increased resources and effective recovery is less straightforward.

The present study focuses on a static resource allocation, where the number and deployment of repair crews remain constant throughout the recovery process. Future research can significantly advance resilience planning by incorporating dynamic resource strategies. The introduction of appropriate thresholds for different damage levels could also be incorporated in the expansion of the characteristic curves, allowing for effective resilience planning.

APPENDIX

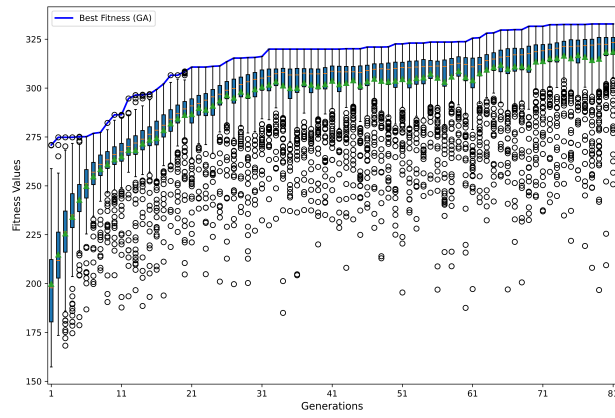


Figure 18: Box-plot of GA training for Network 3 with three crews (repair rate of 75 *m/day*).

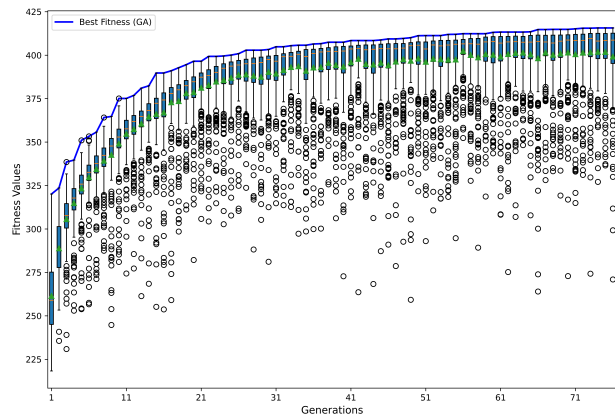


Figure 19: Box-plot of GA training for Network 3 with six crews (repair rate of 150 *m/day*).

Pipe IDs	Length (km)	Pipe IDs	Length (km)
"20"	0.03	"195"	0.01
"40"	0.03	"199"	0.06
"50"	0.03	"201"	0.36
"60"	0.37	"202"	0.03
"101"	4.32	"203"	0.15
"103"	0.41	"204"	1.39
"105"	0.77	"205"	0.40
"107"	0.45	"207"	0.41
"109"	1.20	"209"	0.15
"111"	0.61	"211"	0.20
"112"	0.35	"213"	0.78
"113"	0.51	"215"	0.37
"114"	0.61	"217"	0.16
"115"	0.60	"219"	0.11
"116"	0.50	"221"	0.70
"117"	0.83	"223"	0.35
"119"	0.66	"225"	0.85
"120"	0.22	"229"	1.22
"121"	0.57	"231"	0.19
"122"	0.62	"233"	0.03
"123"	0.61	"235"	0.22
"125"	0.46	"237"	0.36
"129"	0.28	"238"	0.13
"131"	0.98	"239"	0.43
"133"	0.24	"240"	0.15
"135"	0.27	"241"	0.27
"137"	1.98	"243"	0.37
"145"	0.84	"245"	0.30
"147"	0.62	"247"	1.30
"149"	0.42	"249"	0.50
"151"	0.50	"251"	0.62
"153"	1.07	"257"	0.48
"155"	0.67	"261"	0.67
"159"	0.27	"263"	0.59
"161"	0.31	"269"	0.63
"163"	0.36	"271"	0.24
"169"	1.39	"273"	0.15
"171"	1.05	"275"	0.01
"173"	0.63	"277"	0.67
"175"	0.89	"281"	0.13
"177"	0.61	"283"	0.13
"179"	0.13	"285"	0.01
"180"	0.05	"287"	0.42
"181"	0.15	"289"	0.28
"183"	0.18	"291"	0.33
"185"	0.02	"293"	0.33
"186"	0.03	"295"	0.44
"187"	0.39	"297"	0.19
"189"	0.01	"193"	0.01
"191"	0.23	-	-

Table 3: Complete table with pipe name and lengths for Network 3.

References

- [1] National Infrastructure Advisory Council (NIAC), Critical infrastructure resilience: Final report and recommendations, Tech. rep., U.S. Department of Homeland Security, Washington, D.C., visited on 2023-11-14 (2009).
URL <https://www.cisa.gov/resources-tools/resources/niac-critical-infrastructure-resilience-final-report-and-recommendations>
- [2] A. Assad, O. Moselhi, T. Zayed, A New Metric for Assessing Resilience of Water Distribution Networks, *Water* 11 (8) (2019) 1701, number: 8 Publisher: Multidisciplinary Digital Publishing Institute. doi:10.3390/w11081701.
URL <https://www.mdpi.com/2073-4441/11/8/1701>
- [3] O. Kammouh, C. Fecarotti, A. Marandi, A scalable optimization approach to the intervention planning of complex interconnected infrastructures, *Reliability Engineering & System Safety* 250 (2024) 110281. doi:10.1016/j.ress.2024.110281.
URL <https://www.sciencedirect.com/science/article/pii/S0951832024003533>
- [4] E. Arango, M. Nogal, M. Yang, H. S. Sousa, M. G. Stewart, J. C. Matos, Dynamic thresholds for the resilience assessment of road traffic networks to wildfires, *Reliability Engineering & System Safety* 238 (2023) 109407. doi:10.1016/j.ress.2023.109407.
URL <https://www.sciencedirect.com/science/article/pii/S0951832023003216>
- [5] W. Liu, Z. Song, M. Ouyang, J. Li, Recovery-based seismic resilience enhancement strategies of water distribution networks, *Reliability Engineering & System Safety* 203 (2020) 107088. doi:10.1016/j.ress.2020.107088.
URL <https://www.sciencedirect.com/science/article/pii/S0951832020305895>
- [6] E. Todini, Looped water distribution networks design using a resilience index based heuristic approach, *Urban Water* 2 (2) (2000) 115–122. doi:10.1016/S1462-0758(00)00049-2.
URL <https://www.sciencedirect.com/science/article/pii/S1462075800000492>
- [7] E. Creaco, M. Franchini, E. Todini, The combined use of resilience and loop diameter uniformity as a good indirect measure of network reliability, *Urban Water Journal* 13 (2) (2016) 167–181, publisher: IAHR Website eprint: <https://doi.org/10.1080/1573062X.2014.949799>. doi: 10.1080/1573062X.2014.949799.
URL <https://doi.org/10.1080/1573062X.2014.949799>

- [8] T. D. Prasad, S.-H. Hong, N. Park, Reliability based design of water distribution networks using multi-objective genetic algorithms, *KSCE J Civ Eng* 7 (3) (2003) 351–361. doi:10.1007/BF02831784. URL <https://doi.org/10.1007/BF02831784>
- [9] R. Greco, A. Di Nardo, G. Santonastaso, Resilience and entropy as indices of robustness of water distribution networks, *Journal of Hydroinformatics* 14 (3) (2012) 761–771. doi:10.2166/hydro.2012.037. URL <https://doi.org/10.2166/hydro.2012.037>
- [10] P. Singh, A. Gani, Fuzzy concept lattice reduction using shannon entropy and huffman coding, *Journal of Applied Non-Classical Logics* 25. doi:10.1080/11663081.2015.1039857.
- [11] A. Yazdani, R. Otoo, P. Jeffrey, Resilience enhancing expansion strategies for water distribution systems: A network theory approach, *Environmental Modelling and Software* 26 (12) (2011) 1574–1582. doi:10.1016/j.envsoft.2011.07.016.
- [12] F. Meng, G. Fu, R. Farmani, C. Sweetapple, D. Butler, Topological attributes of network resilience: A study in water distribution systems, *Water Research* 143 (2018) 376–386. doi:10.1016/j.watres.2018.06.048.
- [13] M. Herrera, E. Abraham, I. Stoianov, A Graph-Theoretic Framework for Assessing the Resilience of Sectorised Water Distribution Networks, *Water Resour Manage* 30 (5) (2016) 1685–1699. doi:10.1007/s11269-016-1245-6. URL <https://doi.org/10.1007/s11269-016-1245-6>
- [14] Z. Farahmandfar, K. Piratla, Comparative evaluation of topological and flow-based seismic resilience metrics for rehabilitation of water pipeline systems, *Journal of Pipeline Systems Engineering and Practice* 9 (1). doi:10.1061/(ASCE)PS.1949-1204.0000293.
- [15] Z. Han, D. Ma, B. Hou, W. Wang, Seismic Resilience Enhancement of Urban Water Distribution System Using Restoration Priority of Pipeline Damages, *Sustainability* 12 (3) (2020) 914, number: 3 Publisher: Multidisciplinary Digital Publishing Institute. doi:10.3390/su12030914. URL <https://www.mdpi.com/2071-1050/12/3/914>
- [16] Z. Song, W. Liu, S. Shu, Resilience-based post-earthquake recovery optimization of water distribution networks, *International Journal of Disaster Risk Reduction* 74 (2022) 102934. doi:10.1016/j.ijdrr.2022.102934. URL <https://www.sciencedirect.com/science/article/pii/S2212420922001534>
- [17] T. Tabucchi, R. Davidson, S. Brink, Simulation of post-earthquake water supply system restoration, *Civil Engineering and Environmental Systems* Publisher: Taylor & Francis. doi:10.1080/10286600902862615.

URL <https://www.tandfonline.com/doi/full/10.1080/10286600902862615>

- [18] X. Zhao, Z. Chen, H. Gong, Effects Comparison of Different Resilience Enhancing Strategies for Municipal Water Distribution Network: A Multidimensional Approach, *Mathematical Problems in Engineering* 2015 (1) (2015) 438063, eprint: <https://onlinelibrary.wiley.com/doi/pdf/10.1155/2015/438063>. doi: 10.1155/2015/438063.
URL <https://onlinelibrary.wiley.com/doi/abs/10.1155/2015/438063>
- [19] S. E. Chang, M. Shinozuka, Measuring Improvements in the Disaster Resilience of Communities, *Earthquake Spectra* 20 (3) (2004) 739–755, publisher: SAGE Publications Ltd STM. doi:10.1193/1.1775796.
URL <https://doi.org/10.1193/1.1775796>
- [20] G. P. Cimellaro, A. Tinebra, C. Renschler, M. Fragiadakis, New Resilience Index for Urban Water Distribution Networks, *Journal of Structural Engineering* 142 (8) (2016) C4015014, publisher: American Society of Civil Engineers. doi:10.1061/(ASCE)ST.1943-541X.0001433.
URL <https://ascelibrary.org/doi/10.1061/%28ASCE%29ST.1943-541X.0001433>
- [21] S. Nozhati, A resilience-based framework for decision making based on simulation-optimization approach, *Structural Safety* 89. doi:10.1016/j.strusafe.2020.102032.
- [22] K. A. Klise, D. B. Hart, M. Bynum, J. Hogge, T. Haxton, R. Murray, J. Burkhardt, Water network tool for resilience (wntr) user manual: Version 0.2.3, Technical Report EPA/600/R-20/185, U.S. EPA Office of Research and Development, Washington, DC (2020).
- [23] L. A. Rossman, EPANET 2 USERS MANUAL (2000).
URL <https://nepis.epa.gov/Exe/tiff2png.cgi/P1007WWU.PNG?-r+75+-g+7+D%3A%5CZYFILES%5CINDEX%20DATA%5C00THRU05%5CTIFF%5C00001541%5CP1007WWU.TIF>
- [24] J. M. Wagner, U. Shamir, D. H. Marks, Water Distribution Reliability: Simulation Methods, *Journal of Water Resources Planning and Management* 114 (3) (1988) 276–294, publisher: American Society of Civil Engineers. doi:10.1061/(ASCE)0733-9496(1988)114:3(276).
URL <https://ascelibrary.org/doi/10.1061/%28ASCE%290733-9496%281988%29114%3A3%28276%29>
- [25] M. Fragiadakis, S. Christodoulou, D. Vamvatsikos, Reliability Assessment of Urban Water Distribution Networks Under Seismic Loads, *Water Resources Management* 27. doi:10.1007/s11269-013-0378-0.

- [26] M. Fragiadakis, S. Christodoulou, Seismic reliability assessment of urban water networks, *Earthquake Engineering and Structural Dynamics* 43 (3) (2014) 357–374. doi:10.1002/eqe.2348.
- [27] L. Rossman, R. Clark, W. Grayman, Modeling chlorine residuals in drinking-water distribution systems, *Journal of Environmental Engineering* 120 (1994) 803–820. doi:10.1061/(ASCE)0733-9372(1994)120:4(803).
- [28] Delft High Performance Computing Centre (DHPC), DelftBlue Supercomputer (Phase 2), <https://www.tudelft.nl/dhpc/ark:/44463/DelftBluePhase2> (2024).

3

Conclusions

This chapter presents the findings of this research and draws conclusions. Section 3.1 provides answers to the main research question and sub-questions posed at the beginning of this thesis, emphasizing the key insights. Section 3.2 addresses the limitations of this research and finally, Section 3.3 offers a reflective analysis linking the study's findings to the field of construction management engineering.

3.1. Response to Research Questions

In section 1.4 of this thesis 3 research questions were posed to guide the research into responding to the main research question. The main research question was:

Can we provide a scenario - free assessment of the recovery based seismic resilience of WDNs, by the identification of characteristic curves for system recovery?

The first sub-question that was posed was:

What is the appropriate metric for the assessment of the recovery-based seismic resilience of WDNs?

The answer to this question was derived through a literature review. Research in the field of WDN resilience has predominantly focused on two main approaches for developing metrics to quantify resilience. The first involves surrogate metrics based on energy theory, graph theory, or a combination of the two. These methods are computationally efficient and offer insights into network performance; however, they often lack a direct connection to real-world service outcomes. The second approach utilizes simulation-based methods to model the performance of WDNs under disruptive scenarios. These simulations provide a deeper understanding of network behavior and recovery processes, albeit at the cost of increased computational complexity.

This research adopts a simulation-based assessment of resilience, as the simulation of post-earthquake recovery sequences was identified as a gap in the current literature that warrants further exploration. Among the various metrics considered in the existing literature, the Seismic Resilience Index (SRI) introduced by [13] was selected as the most suitable for this study. The SRI is defined as the summation of the network's Satisfaction Degree Index (SDI) over a discrete time period. The SDI represents the average satisfaction level of consumers with the water service, reflecting how effectively the network meets consumer demand at any given time. According to [13], the significant function for WDNs is to satisfy consumer demand. Unlike metrics that focus on the structural reliability, which primarily evaluate the physical attributes of the system, consumer demand provides a functional perspective. It focuses on how effectively the network performs its primary role—meeting the needs of end-users by delivering adequate water supply.

By addressing the first sub-question and selecting the appropriate resilience metric to quantify the resilience of WDN, we establish a foundation for advancing the analysis. This selection allows us to proceed to the second sub-question, which focuses on how to optimize the recovery process of a damaged WDN using the chosen metric.

The second sub-question that was posed was:

How can we optimize the recovery process of the examined WDN under the different stress scenarios and resource constraints?

The answer to this question lies in the development of the optimization model presented in the thesis paper. The proposed model determines the optimal repair sequence for damaged pipelines to maximize network resilience. The selected metric SRI, is used to evaluate the recovery strategies but with a slight modification. To incentivize the selection of recovery strategies that achieve the fastest recovery with the highest consumer satisfaction, the metric is modified in the optimization model. Specifically, the Satisfaction Degree Index (SDI) at each time-step is divided by the time-step itself. This modification penalizes slower recovery strategies by weighting earlier improvements in network performance more heavily. As a result, the optimization algorithm is driven to prioritize strategies that achieve the quickest restoration of services, ensuring that consumer satisfaction is maximized as soon as possible.

The performance of the optimization algorithm is evaluated by comparing it to a fixed recovery strategy predetermined based on standard practices. In the fixed strategy, the sequence of pipe repairs is determined by the average hydraulic head each pipe provides to the network. This approach aligns with common practices in the WDN community. The curve of the SDI generated by the optimization algorithm and the corresponding numerical value of the SRI are juxtaposed with those obtained from the fixed strategy. The comparison highlights the proposed optimization model's enhanced performance, as it results to quicker restoration of the network with higher SRI values.

In terms of computational complexity, the algorithm is tested on networks of varying scales. The results demonstrate promising outcomes, as the optimization algorithm is capable of achieving the optimal solution for small to medium-sized networks. The optimization model is then applied to combinations of different levels of earthquake magnitudes and available resources, to evaluate its performance for different configurations of earthquake hazards. That results of this work provide the answer to the final sub-question.

The third research sub-question was:

How can we extend the results of the optimization process by identifying the characteristic curves of the system?

As discussed in the previous sub-question, the optimization model is applied to various combinations of earthquake magnitudes and available resources. The results are then used to compile the characteristic curves of the network. These curves map the relationships between earthquake magnitude, available recovery resources, recovery rate, and the overall performance metric, the Seismic Resilience Index (SRI). Characteristic curves are intrinsic to a WDN and dependent on its structural properties, such as the number of pipes and junctions, the network's connectivity and topology, and the length and configuration of its pipes. By capturing these aspects, the curves provide valuable insights into the achievable recovery targets, depending on the seismic levels and the available resources for recovery efforts.

The characteristic curves serve several purposes. During an earthquake event, they act as an assessment tool for decision-makers, enabling efficient resource allocation to minimize recovery time and maximize network resilience. In preparation for seismic hazards, these curves can help define the resource requirements and guide strategic investment to improve the robustness and recovery capacity of the network. Additionally, the curves are adaptable to networks of various sizes and complexities, facilitating comparisons and performance benchmarking across different systems. A significant advantage of characteristic curves is their ability to offer a scenario-free assessment of network resilience. By distilling the complex recovery process into a visual representation they provide a practical tool for decision makers. This visual representation of the relationships between performance metrics and recovery dynamics supports both immediate decision-making during emergencies and long-term planning for seismic hazard preparedness.

In conclusion, this research successfully addresses the main question: *Can we provide a scenario-free assessment of the recovery-based seismic resilience of WDNs by identifying characteristic curves for system recovery?*

Through the development of the optimization model and the compilation of characteristic curves, the study provides a way of evaluating and enhancing the resilience of WDNs under seismic hazards. The chosen metric, assesses the resilience of WDN based on a system's function, the satisfaction of consumer demand. The optimization model leverages this metric, modified to prioritize rapid recovery, to determine optimal repair sequences and proves to outperform the benchmark strategy with which it is compared. By applying the model across various earthquake magnitudes and resource scenarios, the results demonstrate the feasibility of constructing characteristic curves, which map the interplay between seismic stress levels, resource availability, recovery rates, and overall resilience. These curves offer a scenario-free assessment of network performance, providing decision-makers with a practical tool for resource allocation during emergencies and strategic planning for seismic preparedness. Ultimately, this work bridges the gap between theoretical resilience metrics and real-world applications, contributing valuable insights and tools to enhance the resilience and recovery of critical water distribution infrastructure.

3.2. Research Limitations

Although this research offers considerable contributions in the assessment and optimization of recovery-based seismic resilience of WDNs, it is important to acknowledge several limitations. First, the proposed optimization model is computationally intensive, particularly for large-scale networks, which may limit its practical application without further refinement or the use of heuristic approaches. Second, the study assumes predefined resource availability and earthquake scenarios, which may not fully capture the uncertainty and variability inherent in real-world conditions. Third, while the characteristic curves provide valuable insights, they are derived based on network-specific properties, meaning their applicability to other networks requires careful adaptation. Lastly, the study does not explicitly account for cascading effects or inter-dependencies with other infrastructure systems, which could significantly influence recovery dynamics in complex urban environments. Addressing these limitations in future work could further enhance the applicability and robustness of the proposed framework.

3.3. Reflection & Connection to the CME program

This reflection aims to highlight the relevance of the research to the field of construction management engineering. The Construction Management and Engineering (CME) master's program at TU Delft emphasizes innovative strategies for managing, maintaining, and optimizing critical infrastructure.

This study on WDNs aligns with the CME program's focus by tackling the challenges of infrastructure resilience and decision-making under uncertainty. Traditional risk management in civil engineering has often concentrated on mitigating risks under predefined scenarios, focusing on expected hazards and their quantifiable consequences [1]. However, this approach falls short in addressing the cases where the hazards cannot be easily quantified, or the adverse consequences are not easily imagined. By shifting to resilience-based strategies, which emphasize the ability of systems to absorb shocks, adapt to changing conditions, and recover functionality swiftly [11], this study embraces a paradigm shift in infrastructure management.

The Seismic Resilience Index (SRI) is chosen as the most suitable metric for evaluating the performance of WDNs under seismic hazards, placing consumer demand at the forefront of resilience assessment. This metric forms the foundation for informed decision-making and aligns with the CME program's emphasis on providing tools to assess and enhance critical infrastructure holistically. The introduction of an optimization model builds upon this metric by providing the optimal repair strategy for the pipeline infrastructure. The model's integration of hydraulic simulations, fragility modeling, and meta-heuristic optimization reflects the interdisciplinary approach championed by the CME program, combining technical expertise with strategic resource management. A key outcome of this work is the development of characteristic curves that capture the dynamic behavior of WDNs under varying stress levels and resource allocations. These curves provide a visual and quantitative representation of recovery trajectories, illustrating the trade-offs between resource availability, recovery speed, and network performance.

For asset managers, these tools are invaluable for making informed decisions about resource allocation, repair prioritization, and long-term investments in retrofitting or upgrading vulnerable components. By

enabling infrastructure professionals to anticipate disruptions and plan effectively, the study supports the CME program's mission to equip future engineers with the knowledge and skills to manage resilient, adaptable, and sustainable infrastructure systems. This synergy underscores the relevance of the research to the program's broader objectives, preparing graduates to tackle the complexities of modern infrastructure management with innovative, resilience-oriented approaches.

References

- [1] Erica Arango et al. “Dynamic thresholds for the resilience assessment of road traffic networks to wildfires”. In: *Reliability Engineering & System Safety* 238 (Oct. 2023), p. 109407. ISSN: 0951-8320. DOI: 10.1016/j.res.2023.109407. URL: <https://www.sciencedirect.com/science/article/pii/S0951832023003216> (visited on 03/28/2024).
- [2] Ahmed Assad, Osama Moselhi, and Tarek Zayed. “A New Metric for Assessing Resilience of Water Distribution Networks”. en. In: *Water* 11.8 (Aug. 2019). Number: 8 Publisher: Multidisciplinary Digital Publishing Institute, p. 1701. ISSN: 2073-4441. DOI: 10.3390/w11081701. URL: <https://www.mdpi.com/2073-4441/11/8/1701> (visited on 02/19/2024).
- [3] Stephanie E. Chang and Masanobu Shinozuka. “Measuring Improvements in the Disaster Resilience of Communities”. en. In: *Earthquake Spectra* 20.3 (Aug. 2004). Publisher: SAGE Publications Ltd STM, pp. 739–755. ISSN: 8755-2930. DOI: 10.1193/1.1775796. URL: <https://doi.org/10.1193/1.1775796> (visited on 04/02/2024).
- [4] G. P. Cimellaro et al. “New Resilience Index for Urban Water Distribution Networks”. EN. In: *Journal of Structural Engineering* 142.8 (Aug. 2016). Publisher: American Society of Civil Engineers, p. C4015014. ISSN: 1943-541X. DOI: 10.1061/(ASCE)ST.1943-541X.0001433. URL: <https://ascelibrary.org/doi/10.1061/%28ASCE%29ST.1943-541X.0001433> (visited on 02/20/2024).
- [5] Enrico Creaco, Marco Franchini, and Ezio Todini. “The combined use of resilience and loop diameter uniformity as a good indirect measure of network reliability”. In: *Urban Water Journal* 13.2 (Feb. 2016). Publisher: IAHR Website _eprint: <https://doi.org/10.1080/1573062X.2014.949799>, pp. 167–181. ISSN: 1573-062X. DOI: 10.1080/1573062X.2014.949799. URL: <https://doi.org/10.1080/1573062X.2014.949799> (visited on 09/23/2024).
- [6] Z. Farahmandfar and K.R. Piratla. “Comparative evaluation of topological and flow-based seismic resilience metrics for rehabilitation of water pipeline systems”. In: *Journal of Pipeline Systems Engineering and Practice* 9.1 (2018). DOI: 10.1061/(ASCE)PS.1949-1204.0000293.
- [7] Royce Francis and Behailu Bekera. “A metric and frameworks for resilience analysis of engineered and infrastructure systems”. In: *Reliability Engineering & System Safety* 121 (Jan. 2014), pp. 90–103. ISSN: 0951-8320. DOI: 10.1016/j.res.2013.07.004. URL: <https://www.sciencedirect.com/science/article/pii/S0951832013002147> (visited on 09/23/2024).
- [8] Zhao Han et al. “Seismic Resilience Enhancement of Urban Water Distribution System Using Restoration Priority of Pipeline Damages”. en. In: *Sustainability* 12.3 (Jan. 2020). Number: 3 Publisher: Multidisciplinary Digital Publishing Institute, p. 914. ISSN: 2071-1050. DOI: 10.3390/su12030914. URL: <https://www.mdpi.com/2071-1050/12/3/914> (visited on 04/02/2024).
- [9] Wei Liu et al. “Recovery-based seismic resilience enhancement strategies of water distribution networks”. In: *Reliability Engineering & System Safety* 203 (Nov. 2020), p. 107088. ISSN: 0951-8320. DOI: 10.1016/j.res.2020.107088. URL: <https://www.sciencedirect.com/science/article/pii/S0951832020305895> (visited on 03/31/2024).
- [10] F. Meng et al. “Topological attributes of network resilience: A study in water distribution systems”. In: *Water Research* 143 (2018), pp. 376–386. DOI: 10.1016/j.watres.2018.06.048.
- [11] National Infrastructure Advisory Council (NIAC). *Critical Infrastructure Resilience: Final Report and Recommendations*. Tech. rep. Visited on 2023-11-14. Washington, D.C.: U.S. Department of Homeland Security, 2009. URL: <https://www.cisa.gov/resources-tools/resources/niac-critical-infrastructure-resilience-final-report-and-recommendations>.

- [12] T. Devi Prasad, Sung-Hoon Hong, and Namsik Park. "Reliability based design of water distribution networks using multi-objective genetic algorithms". en. In: *KSCE J Civ Eng* 7.3 (May 2003), pp. 351–361. ISSN: 1976-3808. DOI: 10.1007/BF02831784. URL: <https://doi.org/10.1007/BF02831784> (visited on 02/26/2024).
- [13] Zhaoyang Song, Wei Liu, and Shihu Shu. "Resilience-based post-earthquake recovery optimization of water distribution networks". In: *International Journal of Disaster Risk Reduction* 74 (May 2022), p. 102934. ISSN: 2212-4209. DOI: 10.1016/j.ijdr.2022.102934. URL: <https://www.sciencedirect.com/science/article/pii/S2212420922001534> (visited on 02/20/2024).
- [14] Taronne Tabucchi, Rachel Davidson, and Susan Brink. "Simulation of post-earthquake water supply system restoration". EN. In: *Civil Engineering and Environmental Systems* (Dec. 2010). Publisher: Taylor & Francis. DOI: 10.1080/10286600902862615. URL: <https://www.tandfonline.com/doi/full/10.1080/10286600902862615> (visited on 04/02/2024).
- [15] Ezio Todini. "Looped water distribution networks design using a resilience index based heuristic approach". In: *Urban Water*. Developments in water distribution systems 2.2 (June 2000), pp. 115–122. ISSN: 1462-0758. DOI: 10.1016/S1462-0758(00)00049-2. URL: <https://www.sciencedirect.com/science/article/pii/S1462075800000492> (visited on 03/26/2024).